Cortana Corporation

520 N. Washington Street, Falls Church, VA 22046-3538 Tel: 703 534-8000
Fax: 703 534-8005 E-mail: corporate@cortana.com

An Empirical Model-Based MOE for Friction Reduction by Slot-Ejected Polymer Solutions in an Aqueous Environment

Issue Date: 21 December 2007

Prepared by: Dr. John G. Pierce

Under Contract No.: N00014-06-C-0535

Submitted to: Office of Naval Research
Dr. Paul Rispin, Code 333
One Liberty Center
875 N. Randolph St.
Arlington, VA 22203-1995

Report Documentation Page

Form Approved
OMB No. 0704-0188

1. REPORT DATE	2. REPORT TYPE	3. DATES COVERED
21 DEC 2007		**00-00-2007 to 00-00-2007**

4. TITLE AND SUBTITLE	5a. CONTRACT NUMBER
An Empirical Model-based MOE for Friction Reduction by Slot-Ejected Polymer Solutions in an Aqueous Environment	5b. GRANT NUMBER
	5c. PROGRAM ELEMENT NUMBER
6. AUTHOR(S)	5d. PROJECT NUMBER
	5e. TASK NUMBER
	5f. WORK UNIT NUMBER
7. PERFORMING ORGANIZATION NAME(S) AND ADDRESS(ES) **Cortana Corporation,520 N Washington Street,Falls Church,VA,22046-3538**	8. PERFORMING ORGANIZATION REPORT NUMBER
9. SPONSORING/MONITORING AGENCY NAME(S) AND ADDRESS(ES)	10. SPONSOR/MONITOR'S ACRONYM(S)
	11. SPONSOR/MONITOR'S REPORT NUMBER(S)

12. DISTRIBUTION/AVAILABILITY STATEMENT
Approved for public release; distribution unlimited

13. SUPPLEMENTARY NOTES

14. ABSTRACT

15. SUBJECT TERMS

16. SECURITY CLASSIFICATION OF:			17. LIMITATION OF ABSTRACT	18. NUMBER OF PAGES	19a. NAME OF RESPONSIBLE PERSON
a. REPORT **unclassified**	b. ABSTRACT **unclassified**	c. THIS PAGE **unclassified**	**Same as Report (SAR)**	**57**	

Table of Contents

1 Introduction

Since the discovery of the Toms Effect in 1948, many investigators have explored the nature and causes of polymer-induced friction reduction, using both experimental and theoretical methods.

Experimental investigations have focused on four related but distinct cases: (1) internal friction reduction produced by a dilute polymer solution of uniform concentration flowing through a pipe; (2) internal friction reduction produced by a uniform concentration of polymer between two rotating cylinders (Couette flow); (3) external friction reduction produced by a uniform concentration of polymer ('polymer ocean') flowing along a flat plate or body of revolution; (4) external friction reduction produced by a non-uniform concentration of polymer ejected into the flow at defined locations along a flat plate or body of revolution.

Theoretical investigations fall into two general categories: (1) phenomenological models that describe the essential features of the experimental results in broad general terms; (2) physics models that attempt to explain the friction reduction effect using fundamental principles of hydrodynamics and the physical characteristics of the polymers. The physics models include both analytical models and numerical simulations.

To date, the theoretical investigations are, at best, only partly successful. Some of the phenomenological models accurately capture some aspects of the experimental observations. The numerical simulations also succeed in replicating some experimental measurements. However, there is still no comprehensive understanding of the mechanisms of polymer-induced friction reduction, and, in more practical terms, there are no good models that capture enough detail to be useful for engineering design of functional drag-reduction systems employing slot-ejected polymer where the polymer concentration varies substantially downstream from the slot.

External friction reduction for use on submarines and other marine vehicles is an area of great practical importance. In such applications, the polymer must be ejected at one or more locations along the vehicle's exterior surface, so the effects of non-uniform polymer concentration are paramount. Consequently, a model that can describe and predict friction reduction produced by slot-ejected polymer along an external surface would be very useful for system engineering.

This paper describes a preliminary version of such a model. This model has been created by assembling partial models published by other investigators and by exploiting published data to infer additional phenomenology. Experiments involved cover Professor Virk's work published in 1970; the work of the Tulin team at Hydronautics through the 1970's; Vdovin & Smol'yakov in the late 1970's and early 1980's; Povkh & Pogrebnyak from 1979 through 1998; Smith and Perkins in the mid-1990's; Deutsch, Petrie, Fontaine & Brungart from the 1990's to the present, including work with Cortana Corporation; and, most recently, work by Ceccio and his team (2006).

Results from this model are compared to other experiments that were not used for model development. Such comparisons provide limited validation of the model, but also indicate areas where improvement is needed.

This model will be useful for several purposes.

- Enhanced understanding of measurements from slot-ejected polymer experiments
- System design for slot-ejected polymer friction reduction on marine vehicles
- Specification of new experiments to improve phenomenological component models
- Identification of areas for more focused theoretical investigations.

2 Definition of Concepts and Terminology

Flow is assumed along a solid surface. Initially the surface is treated as a flat plate with finite *length*, L_p, in the direction parallel to the flow. The surface is assumed to be of infinite extent in the direction perpendicular to the flow, making the problem two-dimensional in Cartesian geometry. Later versions of the model may be generalized to a body of revolution, also having length, L_p. In that case, the problem would be two-dimensional in cylindrical geometry.

The flow is characterized by the *free-stream velocity*, U_∞. The free-stream velocity is parallel to the surface of the plate or to the axis of revolution of the body.

The flowing fluid, called the *solvent*, is characterized by its *density*, ρ, and its *kinematic viscosity*, ν. Alternatively, the *dynamic viscosity*, $\mu = \nu\rho$, may be used as a descriptor. Both of these parameters are functions of temperature and salinity of the solvent, but, to first order, are treated just as constants of the material.

In the vicinity of the surface, the flow is characterized by a *boundary layer*. At the leading edge of the plate or body, the boundary layer may be a *laminar boundary layer*. Some distance downstream the flow makes a transition from laminar to turbulent, and the boundary layer becomes a *turbulent boundary layer*. In most applications, the flow of interest for purposes of friction reduction is turbulent. In some experiments the boundary layer may be intentionally tripped by the experimenter to make it turbulent. The position, x, along the plate at which the turbulent boundary layer begins is called the *virtual origin* of the boundary layer. The virtual origin is assigned the coordinate $x = 0$, and downstream positions are referenced to that origin.

A common non-dimensional descriptor of the flow is the *Reynolds number*. Because a length scale enters into the Reynolds number, confusion can arise among Reynolds numbers referenced to different length scales. In the problem to be considered here, both the plate length and the longitudinal coordinate of the boundary layer play roles. The two associated Reynolds numbers are distinguished by subscripts.

$$Re_L = U_\infty L_p/\nu \qquad (1)$$

$$Re_x = U_\infty x/\nu. \qquad (2)$$

The experimental literature also includes Reynolds numbers that are defined on the basis of boundary layer thickness and/or diameter (in the case of pipe flow). Care must be exercised to distinguish among these various Reynolds numbers.

Within the turbulent boundary layer there are distinguishable structures. A *viscous sub-layer* extends out a small distance from the solid surface. In the viscous sub-layer, viscous forces are much larger than inertial forces. The longitudinal velocity is zero at the wall (no-slip condition), and increases, first linearly across the viscous sub-layer, then

as some power of distance from the wall. In the outer part of the boundary layer, inertial forces are much larger than viscous forces, and the latter can be neglected. The velocity profile in that region is a logarithmic function of distance from the wall; the velocity approaches the free-stream velocity at the outer edge of the boundary layer. Between these two sub-layers is a *transition* or *buffer layer* in which viscous forces and inertial forces are comparable in magnitude. In this report, the near-wall region is considered to include the viscous sublayer and the buffer layer.

Polymer solutions are ejected into the external flow through one or more *slots* in the solid surface, or, less commonly, through *pores*. In keeping with the two-dimensional geometry, the slot is assumed to extend indefinitely in the direction perpendicular to the flow. Quantitative descriptors are then referenced to a unit span of the slot.

The streamwise coordinate of the slot is x_0, referenced to the virtual origin of the boundary layer. The downstream distance from the slot, which is used in much of the analysis, is designated as x_s. Thus,

$$x = x_0 + x_s. \tag{3}$$

The performance of the slot is characterized by the *ejection angle*, ϕ, and by the *volume ejection rate per unit span*, q. An alternate description is provided by the *ejection velocity*, u_{ej}, which is related to q and to the *slot width*, w_s, by

$$q = w_s\, u_{ej}. \tag{4}$$

Since q has the dimensions (Volume/Time)/Span ~ Length^2/Time, it is often referenced to a multiple of the kinematic viscosity which has the same dimensions. The quantity

$$Qs \equiv 67.3\, \nu \tag{5}$$

is the volume transport rate per unit span of the flow in the viscous sub-layer of an idealized model (from the wall out to 11.6 viscous wall units). By convention it is often used as the reference for the volume ejection rate of the slot; q is expressed as a multiple of Qs.

$$q = n\, Qs. \tag{6}$$

The ejected *solute* (polymer) is characterized by its *initial concentration* c_0, expressed in grams/cc or in *weight parts per million* (*wppm*). Other molecular properties of the polymeric material are often used in physics-based modeling but rarely in phenomenological modeling.

The *friction reduction*, DR, is the fractional change in drag in the presence of polymer ($C_{f0} - C_{fp}$) relative to the drag in the absence of polymer (C_{f0}).

$$DR = (1 - C_{fp}/C_{f0}). \tag{7}$$

Contemporary measurement technology allows measurement of drag over a small localized area. Thus, friction reduction can be a local variable

$$DR = DR(x_s), \tag{8}$$

measured with respect to the ejection slot. When the local value is known, an integrated effective friction reduction can be calculated.

Finally, much of the literature on friction reduction by slot-ejected polymers uses a dimensionless group called the *K factor*. This factor is defined as

$$K \equiv qc/\rho U_\infty x_s. \tag{9}$$

This dimensionless group can be factored into other dimensionless groups in a variety of ways. One factorization emphasizes mass flux and Reynolds number:

$$K = (qc/\mu)(1/Re_{xs}) \tag{10}$$

Another factorization emphasizes ratios of dimensionally similar fundamental quantities.

$$K = (c/\rho)(u_{ej}/U_\infty)(w_s/x_s) \tag{11}$$

Measured values of friction reduction are often expressed as functions of K. One of the goals of phenomenological modeling is to fully explain the observed relationship between $DR(x_s)$ and $K(x_s)$.

3 Prior Work

Two key papers on slot-ejected polymers were published by Vdovin & Smol'yakov in 1978 and 1981.

The central thesis of these papers is that diffusion alters the mean wall concentration of polymer as a function of distance from the slot in repeatable and statistically predictable ways. They introduced the concept of diffusion length, L, defined as the downstream distance at which the wall concentration drops to 1/e of its initial value. For their experiments free stream velocities ranged between 2.5 and 10 m/s. Ejection flow rates ranged between 0.77 and 15.4 cm^2/s (1.14 Qs to 22.88 Qs).

Vdovin & Smol'yakov established several properties of the diffusion length.

- When the ejection angle is small ($\leq 7^\circ$), L is independent of the free stream velocity. It was found to depend only on the dimensionless group qc_0/μ. For small values of qc_0/μ (<10), L is proportional to qc_0/μ. For larger values of qc_0/μ, L approaches a maximum value of ~ 70 cm.

- When the ejection angle is larger (~20°), L does depend on the free stream velocity. At an ejection angle of 20° experiments on several different polymers showed that

$$L = k\,(qc_0/\rho U_\infty) \qquad (12)$$

  over the full range of measurements. The parameter k was found to be characteristic of the polymer type, with $k_{ref} = 6.25 \times 10^6$ being the reference value for PEO WSR-301. For other polymers, k is expressed as $k = k_0 k_{ref}$. Although no limiting value was measured up to $L \sim 200$ cm, they did not rule out the possibility of L reaching an asymptotic value for very large values of $qc_0/\rho U_\infty$.

These observations of Vdovin & Smol'yakov suggest that the ejection angle plays a key role in the downstream behavior of the polymer. For small ejection angles, the polymer stays close to the surface so that its behavior is governed by inner variables q, c_0, ρ, ν. For larger ejection angles, the polymer extends further into the boundary layer, or may actually penetrate the boundary layer, so that the outer variable U_∞ becomes important as well.

As discussed by Vdovin & Smol'yakov, the diffusion length is to be interpreted in the context of three 'zones' downstream of the ejection slot. The *initial zone* is very close to the slot, the solute is confined to the near-wall region, and the wall concentration remains close to the initial concentration. Typically the initial zone is very short. In the *intermediate zone*, the diffusion process transports the solute away from the wall until it occupies much of the turbulent boundary layer. The concentration at the wall decreases

exponentially in this zone. Finally, in the *far zone*, as the boundary layer expands downstream, diffusion continues to reduce the wall concentration, but the rate is algebraic rather than exponential.

Vdovin & Smol'yakov provide analytical models for the wall concentration in the intermediate and far zones. Those models are based on fitting a large amount of experimental data.

In the intermediate zone

$$c_w/c_0 \sim \exp(-\alpha x/L - \beta), \tag{13}$$

where α is a parameter that depends on the angle at which the ejectant is introduced into the flow, and $\beta = 1 - \alpha$, which ensures that $c_w/c_0 = 1/e$ when $x = L$. Only two ejection angles were tested by the authors. They found that for $\phi = 7^\circ$, $\alpha = 0.7$ and for $\phi = 20^\circ$, $\alpha = 1.8$. Note that c_w depends on c_0 both explicitly and, through L, implicitly.

In the far zone their data fit an algebraic expression of the form

$$c_w/\rho = 4.16\ 10^{-5}\ (x/L)^{-1.38}. \tag{14}$$

[Note: Vdovin & Smol'yakov (1981) contains an apparent typographical error. Here 10^{-5} has been substituted for their 10^{-2} to make the equation agree with Figure 5 of that paper.] In this case c_w does not depend explicitly on the initial concentration, but it depends implicitly on q, c_0, and U_∞ through L.

4 Model Development

The model presented herein incorporates three primary features.

- The relationship between wall concentration of the polymer and the distance from the slot. This relationship is taken directly from Vdovin and Smol'yakov (1981), with allowance for blending the appropriate functions between the different diffusion zones.

- The relationship between wall concentration and friction reduction. For small concentration values, an empirical relationship is developed in this paper on the basis of data published by Petrie *et al* (2003). For large concentration values, an approximate analytical formula is based on observations of Wu & Tulin (1972), Wu, Fruman, & Tulin (1977) and Povkh *et al* (1980).

- The maximum friction reduction as a function of Reynolds number. For this calculation the local friction coefficient for pure solvent C_{f0} was taken from the empirical function cited by White (1991). That function was found to agree very closely with a different empirical function cited by Schlichting (1960). The local friction coefficient for maximum friction reduction C_{fp} was taken from Winkel *et al* (2006) citing Virk *et al* (1970).

These three basic features were supplemented by simple subsidiary calculations: the relationship between K and x/*L*, taking account of possible saturation of *L*; the relationship between K and Re_x, taking account of the distance between the slot and the virtual origin of the boundary layer.

These components of the model are described in the next sections.

4.1 *Wall Concentration vs. x/L*

In the initial zone, we assume

$$c_w = c_0. \tag{15}$$

In the intermediate zone we use the formula of Vdovin & Smol'yakov

$$c_w = c_0 \exp(-\alpha x/L - \beta). \tag{16}$$

In the far zone we use the formula of Vdovin & Smol'yakov

$$c_w = \rho\, 4.16\, 10^{-5}\, (x/L)^{-1.38}. \tag{17}$$

To blend these formulas for the different zones, we multiply by functions that roll-off sharply. The parameter XOL1 = .5 is introduced as an operator-selectable parameter. The roll-off function is $\exp(-((x/L)/XOL1)^2)$.

Then, in the initial zone

$$c_1 = c_0 \exp(-((x/L)/XOL1)^2). \quad (18)$$

In the intermediate zone

$$c_2 = c_0 \exp(-\alpha x/L - \beta)(1 - \exp(-((x/L)/XOL1)^2). \quad (19)$$

In the far zone

$$c_3 = \rho\, 4.16\, 10^{-5}\, (x/L)^{-1.38}(1 - \exp(-((x/L)/XOL1)^2). \quad (20)$$

Each of these functions has the proper roll-off behavior, so that the sum

$$c_w = c_1 + c_2 + c_3 \quad (21)$$

provides a smooth transition between zones and reflects the desired behavior in each zone.

4.2 *Friction Reduction vs. Wall Concentration*

The dependence of friction reduction on the wall concentration is an important issue. The model depends in a sensitive way on the functional relationship between the two variables. Data to establish such a relationship is most productively obtained from pipe flow experiments or from polymer ocean experiments in which the concentration is uniform and presumably known with reasonable accuracy. One must then assume that the relationship continues to hold in slot ejection experiments where the wall concentration varies with x_s and other parameters.

Vdovin and Smol'yakov present a functional form for pipe flow.

$$DR = 2.49 + 0.35 \log_{10}(k_0 c/\rho). \quad (22)$$

However, they qualify this expression by noting that it holds only over limited range of the product $k_0 c/\rho$ (2×10^{-7} to 4×10^{-6}), essentially equivalent to a concentration less than 4 wppm. They do not note any dependence on Reynolds number or other parameters.

In practice it is well known that there is a maximum friction reduction that is a function of Reynolds number. The actual friction reduction approaches that limit rather quickly as the polymer concentration increases from zero. The maximum friction reduction may be achieved over a finite range of concentration values, but, as the concentration continues

to increase, the friction reduction again decreases. Any realistic model should incorporate those features.

4.2.1 Low Concentration Limit

A recent paper by Petrie *et al* (2003) contains some useful data on the functional relationship between concentration and friction reduction at the lower concentration values. Although the main thrust of that paper is on the effects of surface roughness, it does present baseline data for the flow of a polymer ocean across a smooth flat plate. The data include variations in both polymer concentration and Reynolds number. Data extracted from the "Figure 5" paper of Petrie *et al* are shown in the following graph, refer to Figure 1.

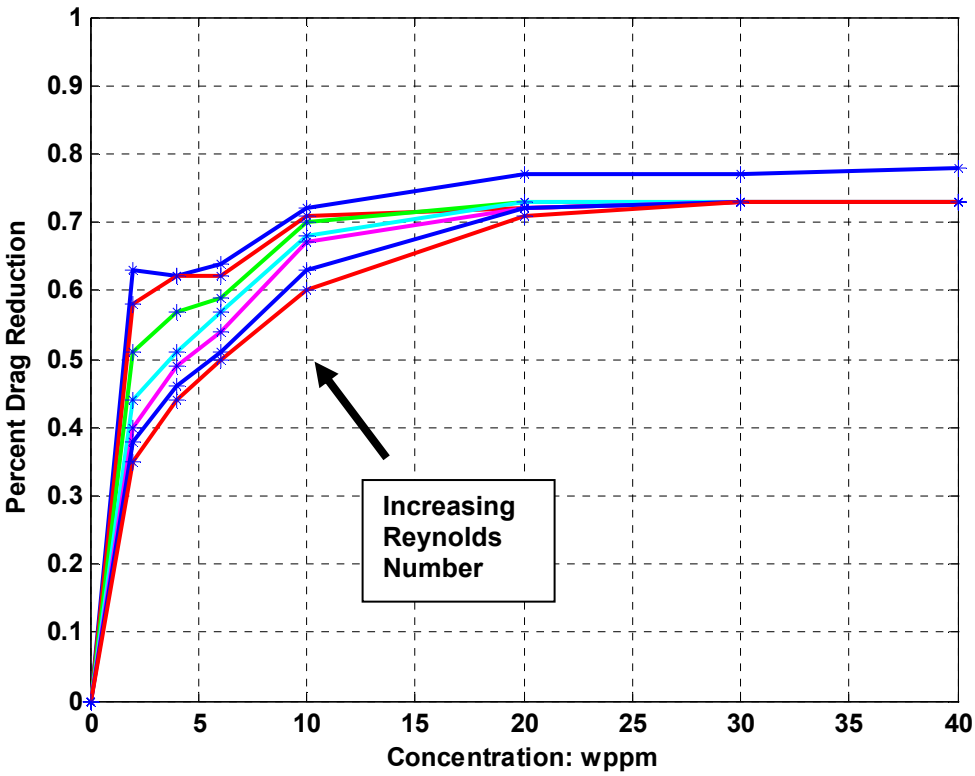

Figure 1: Petrie, et al. data for various Reynolds Numbers: 4e6 < Re < 1.1e7

Key features of Figure 1 are that (a) the friction reduction approaches saturation rapidly, essentially achieving maximum friction reduction for c ~ 20 wppm; (b) the rate at which friction reduction approaches its asymptote depends on the Reynolds number, with the largest Reynolds numbers corresponding to the most rapid growth in friction reduction.

It would be tempting to model the approach to saturation as a simple exponential:

$$DR(c) = DR_{max}(1 - \exp(-\gamma c)), \qquad (23)$$

where γ is a constant that may depend on the Reynolds number. Closer examination shows that this is not necessarily a good model. The friction reduction rises very rapidly for small values of c, and then approaches the asymptote more slowly than would a simple exponential. A more reasonable model that has the desired properties is

$$DR(c) = DR_{max}(1 - \exp(-\gamma(Re)c^{\beta\beta})), \tag{24}$$

where $\beta\beta$ is a constant of less than one and γ appears to depend on flow velocity.

Least squares fits to the data of Petrie *et al* for each Reynolds number shows that $0.4 < \beta\beta < 0.6$, with no systematic dependence of $\beta\beta$ on Reynolds number. The mean value over the range of Reynolds numbers is $<\beta\beta> = 0.54$. The coefficient γ does depend on the flow velocity in a systematic way. A least squares fit for that parameter gives

$$\gamma = 1.05\ (Re_{ref}/Re)^{.83}. \tag{25}$$

Consequently, the scaling $c^{0.54}/Re^{0.83}$ should collapse the data. Figure 2 shows this scaling. The function $1 - \exp(-1.05(Re_{ref}/Re)^{0.83}c^{0.54})$ is shown for comparison.

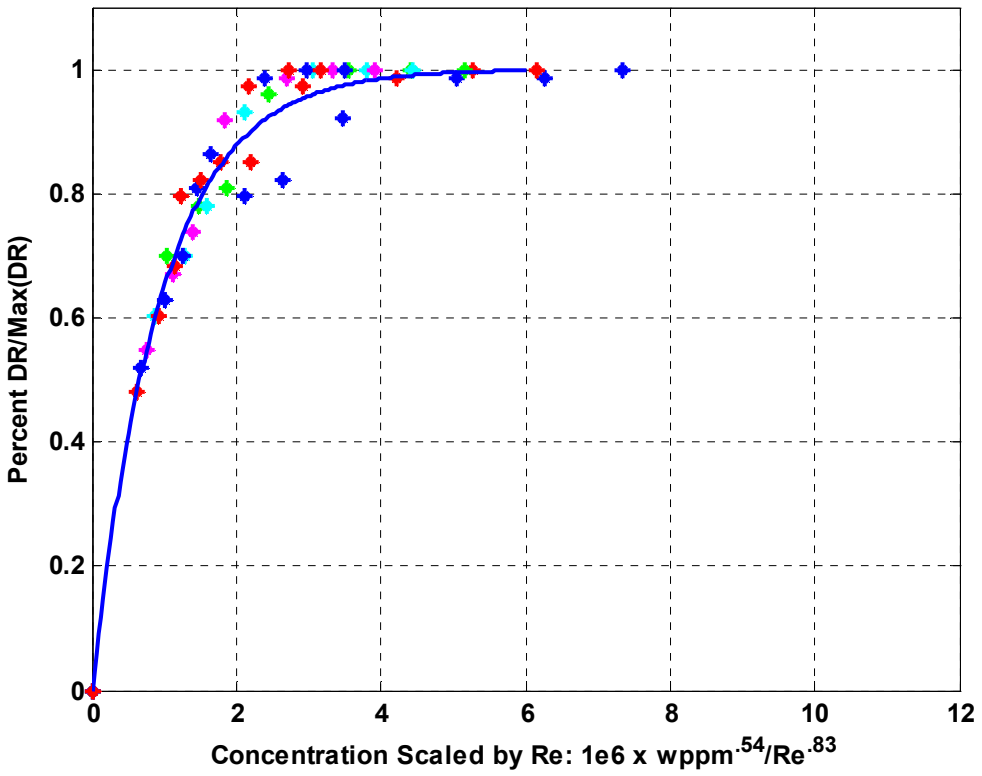

Figure 2: Petrie, et al. scaled data for various Reynolds numbers: 4e6 < Re < 1.1e7

An important aspect of the data of Petrie *et al* is that they used Re_L, not Re_x for the Reynolds number. Thus, the only variable factor in their Reynolds number is the velocity, so the friction reduction scaling could be written instead as

$$(U_{ref}/U_\infty)^{0.83} c^{0.54}. \qquad (26)$$

This form emphasizes that concentration and velocity scale with different exponents. As a consequence, the K factor, in which c and $1/U_\infty$ appear with the same exponent, cannot be expected to completely collapse the data.

Extraction of scaling exponents from the data of Petrie *et al* is rather crude, and the exact values of the exponents may vary. Clearly, a much larger set of polymer ocean data would be needed to arrive at a fully reliable estimate.

Two sets of pipe flow data support an estimate of $\beta\beta \approx .5$. Unfortunately, those data sets do not contain information on the concurrent effects of varying concentration and velocity (or Reynolds number). Virk & Baher (1970) found an effect proportional to $c^{½}$ over two orders of magnitude in the variation of c. Data from Warholic *et al* (1999) is shown in Figure 3. The best fit to that data at $Re \approx 20{,}000$ gives $\beta\beta = 0.527$.

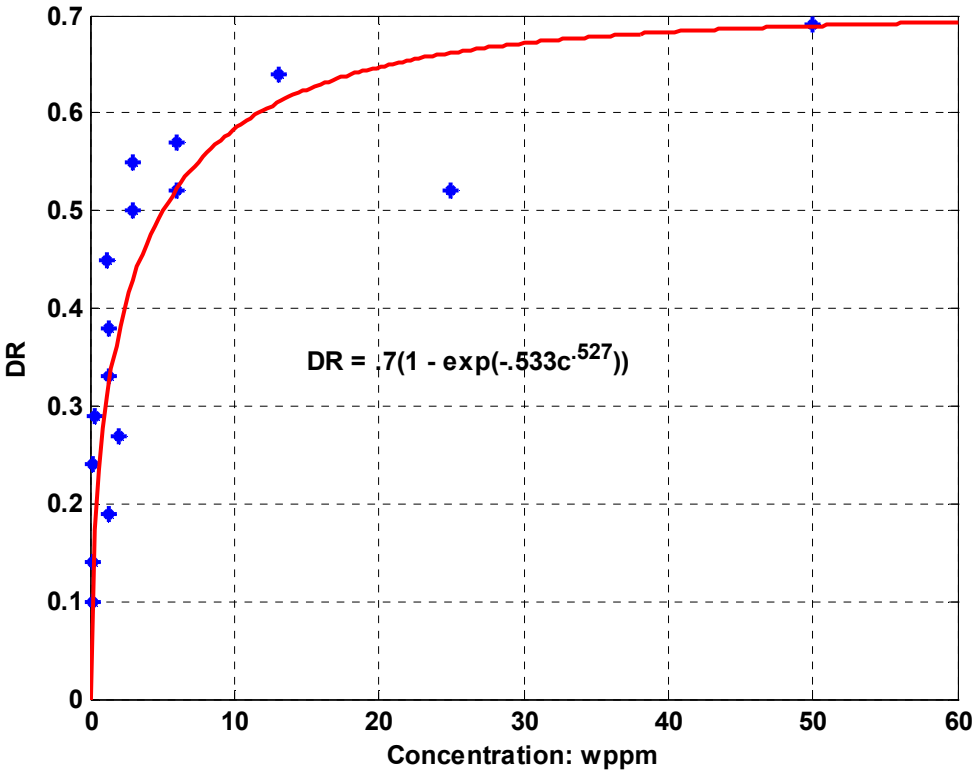

Figure 3: Data from Warholic, et al. (1999)

In the present model, the friction reduction will be incorporated as

$$DR = DR_{max} (1 - \exp(-\gamma(U_{ref}/U_\infty)^{\delta} c^{\beta\beta})), \quad (27)$$

with nominal values $\gamma = 1.05$, $\delta = 0.83$, $\beta\beta = 0.54$, and $U_{ref} = 457$ cm/sec estimated from Petrie *et al*. ($\beta\beta$ is used here to distinguish this parameter from the β used by Vdovin & Smol'yakov.) DR_{max} is a function of Reynolds number, as discussed in Section 4.3.

4.2.2 High Concentration Limit

Wu & Tulin (1972) first showed that friction reduction performance decreases for high concentrations of polymer. For a polymer ocean flowing along a flat plate, they showed that maximum friction reduction occurred for c ~ 100 wppm. For slot ejection into a flow with $U_\infty = 8$ ft/sec, they showed that integrated friction reduction for the whole plate increased with concentration up to c ~ 500 wppm, then remained constant up to the limits of their experiment at c = 1000 wppm. Subsequent slot-ejection work (Wu, Fruman & Tulin, 1977) extended the concentration range to 5000 wppm. That work showed decreased friction reduction at the end of the approximately 3-meter plate for 1000, 3000, and 5000 wppm, compared to best performance in the range 250 – 500 wppm.

Povkh *et al* (1979) used small diameter tubes to measure friction reduction for various concentrations and various molecular weights of PEO WSR 301. For the molecular weight $M = 10^6$, roughly comparable to that of the polymer used by Wu & Tulin, they also found the maximum friction reduction to occur at c ~ 100 wppm. However, the decrease in friction reduction at higher concentrations was somewhat slower than that reported by Wu & Tulin. They also noted a weak dependence of the optimum concentration on Reynolds number.

Both sets of data are rather sparse. An approximate model for the high concentration behavior, without consideration of the effects of molecular weight or Reynolds number is:

$$DR = DR_{max} (c_{roll}/(c + c_{roll})), \quad (28)$$

where the roll-off concentration, c_{roll}, is an empirical parameter. A value of $c_{roll} \sim 3500$ wppm is used in the present illustration of the model. That value gives a reasonable fit to the data of Povkh *et al*, but overestimates the data of Wu & Tulin. In the implementation of the model, c_{roll} is an operator-selectable parameter.

Combination of the low-concentration and high-concentration models gives the final version used in the present calculations:

$$DR = DR_{max} (1 - \exp(-\gamma(U_{ref}/U_\infty)^{\delta} c^{\beta\beta}))(c_{roll}/(c + c_{roll})). \quad (29)$$

4.3 *Maximum Friction reduction*

Many experiments in different experimental configurations have shown that there is a limiting (minimum) friction factor, C_{fp}, that can be achieved by the use of polymer solutions. That limit is a function of Reynolds number. Similarly, the friction factor in the absence of polymer, C_{f0}, is also a function of Reynolds number.

The maximum friction reduction is

$$DR_{max}(Re_x) = 1 - C_{fp}(Re_x)/C_{f0}(Re_x). \quad (30)$$

The friction factors are available as empirical functions estimated from extensive experimental data. C_{f0} is given as an explicit function by White (1991)

$$C_{f0} = 0.455/(\log_e(0.06Re_x))^2. \quad (31)$$

An alternative empirical function given by Schlichting (1960) produces a nearly identical numerical result over the range of Reynolds numbers of interest.

$$C_{f0} = (2\log_{10}(Re_x)-0.65)^{-2.3}. \quad (32)$$

The expression from White is used in the present model.

C_{fp} is given implicitly by a function cited by Winkel *et al* (2006) referring to the work of Virk *et al* (1970).

$$C_{fp}^{-1/2} = 19\log_{10}(C_{fp}\,Re_x) - 38.1 \quad (33)$$

In this model C_{fp} is calculated as a function of Re_x by fixed point iteration of this equation. Note that this is different from the conventional formula for the Virk asymptote in pipe flow which is based on the diametral Reynolds number Re_D, not Re_x. It is also important to note that the empirical Virk asymptote is based on studies of shear flow. Topologically, turbulent shear flow is ~50% extensional flow and ~50% rotational flow. A different type of flow, in which the proportions of extensional and rotational flows differ, might have a different maximum friction reduction asymptote.

4.4 *Other Functions*

Two final relationships are needed to close the model. It is desired to express the results in terms of the K factor. The wall concentration is expressed in terms of the ratio x_s/L in the formulas of Vdovin & Smol'yakov. The maximum friction reduction is expressed in terms of the Reynolds number Re_x, based on distance from the virtual origin of the boundary layer. It is necessary to relate K to Re_x and x_s/L.

4.4.1 K vs x_s/L

The relationship between K and x_s/L recognizes the possibility that L may reach some upper limit L_{max}. By definition

$$K = qc_0/\rho U_\infty x_s \tag{34}$$

Multiplication by $1 = (L/L)(L_{max}/L_{max})$ gives $K = (L/x_s)\,(L_{max}/L)\,(qc_0/\rho U_\infty L_{max})$.

When $qc_0/\rho U_\infty$ is small, L is proportional: $L = k\, qc_0/\rho U_\infty$. If L approaches an asymptotic value L_{max} when $qc_0/\rho U_\infty$ becomes large, L can be modeled as

$$L = L_{max}\,(1 - \exp(-k\, qc_0/\rho U_\infty L_{max})). \tag{35}$$

Then x_s/L can be written

$$x_s/L = (1/kK)\,F, \tag{36}$$

where the correction factor F is

$$F = (kqc_0/\rho U_\infty L_{max})/\,(1 - \exp(-kqc_0/\rho U_\infty L_{max})). \tag{37}$$

When $kqc_0/\rho U_\infty L_{max}$ is small, $F = 1$, $x_s/L = (1/kK)$, and no correction is necessary. When $kqc_0/\rho U_\infty L_{max}$ becomes large, $F \rightarrow kqc_0/\rho U_\infty L_{max}$ and additional factors of q, c_0, and $1/U_\infty$ are introduced into x_s/L.

4.4.2 K vs. Re_x

The principal distinction here is the choice of origins for K and Re_x. K is referenced to the position of the slot and Re_x is referenced to the virtual origin of the turbulent boundary layer. Since $x = x_0 + x_s$, multiplication by U_∞/ν gives

$$Re_x = Re_{x0} + (qc_0/\mu)(1/K), \tag{38}$$

where $Re_{x0} = U_\infty x_0/\nu$ is the Reynolds number based on the distance from the virtual origin of the boundary layer to the slot. This number will obviously change with flow velocity, and, depending on the location of the slot, can become quite significant.

4.5 *Documentation*

The complete model is coded in MatLab. In the model, all units are cgs, so distances are in centimeters and velocities are in centimeters per seconds.

5 Behavior of the Model

The model requires a large number of inputs. These can be grouped into three categories: (1) established physical parameters: ρ, ν, μ that characterize the solvent; (2) empirical parameters based on prior experiments: k_0, k_{ref}, L_{max}, U_{ref}, the reference velocity in Petrie's experiments, the parameters used to fit the data of Petrie *et al*, γ, δ, $\beta\beta$, and c_{roll}, the parameter used to fit the high concentration behavior; (3) experimental parameters that characterize a specific experiment: free stream velocity U_∞, initial concentration c_0, ejection angle parameter α, ejection rate q, and position of the slot with respect to the virtual origin of the turbulent boundary layer x_0. The first group can be taken as fixed parameters that do not affect the functioning of the model. The second group needs to be investigated to determine the sensitivity of the model to the empirical parameters. Although the empirical parameters have been fit to prior experimental data, it is still necessary to evaluate them and ensure that the results of the model are consistent with new experiments. This process can be viewed as a form of validation. Finally, the model can be used to investigate variations in the experimental conditions expressed by the third group of parameters.

5.1 *Sensitivity to Empirical Parameters*

In this section, we choose a nominal set of parameters and operating conditions as a baseline, and then investigate the sensitivity of the model to the empirical parameters, one-by-one. The joint sensitivities of pairs of parameters will be considered in the future.

The nominal operating conditions are:

U_∞ = 900 cm/sec;
c_0 = 1000 wppm;
q = 5 Qs;
α = 1.8 (slot angle = 20°);
x_0 = 70 cm.

The nominal empirical parameters are

k_0 = 1 (PEO WSR-301);
k_{ref} = 6.25 x 10^6;
L_{max} = 270 cm;
U_{ref} = 457 cm/sec;
γ = 0.80;
δ = 0.83;
$\beta\beta$ = 0.54;
c_{roll} = 3500 wppm

Figure 4 shows the friction reduction as a function of K for the nominal case.

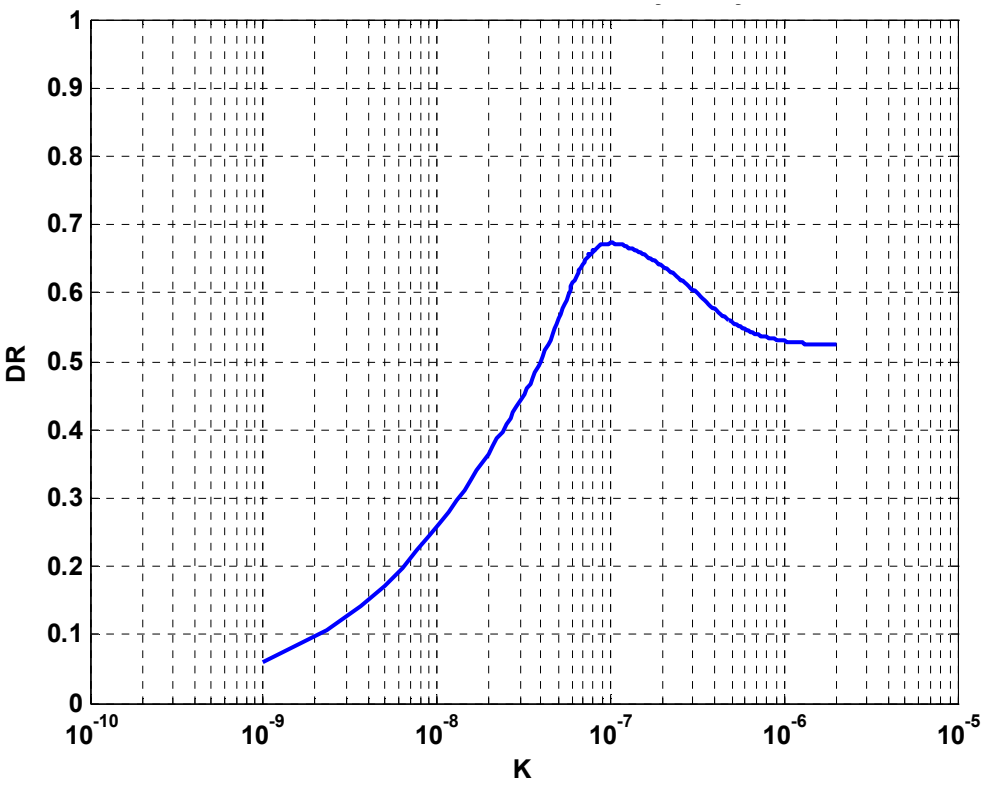

Figure 4: Nominal baseline for sensitivity analysis

Figure 4 is typical of experimental data from slot-ejected polymer experiments. The friction reduction is insignificant for $K < 10^{-9}$. It increases steadily and is more or less proportional to $\log_{10}(K)$ in the range $10^{-8} < K < 10^{-7}$. It then reaches a plateau and may decline in the near-slot region.

The factors that contribute to this shape are shown in Figure 5. Contributions from the initial zone, the intermediate zone, and the far zone are compared with the maximum friction reduction predicted by Virk's asymptote. For this particular set of operating conditions, the contribution from the far zone is equal to the contribution from the intermediate zone at $K \sim 6 \times 10^{-8}$. For smaller values of K, the far zone dominates. For larger values of K, where the contributions from the intermediate and initial zones might be expected to dominate, Virk's asymptote is a governing factor. In this specific example, the intermediate zone has a significant influence only over a very limited range of K. In the initial zone, the influence of the decrease in performance due to high polymer concentration is apparent.

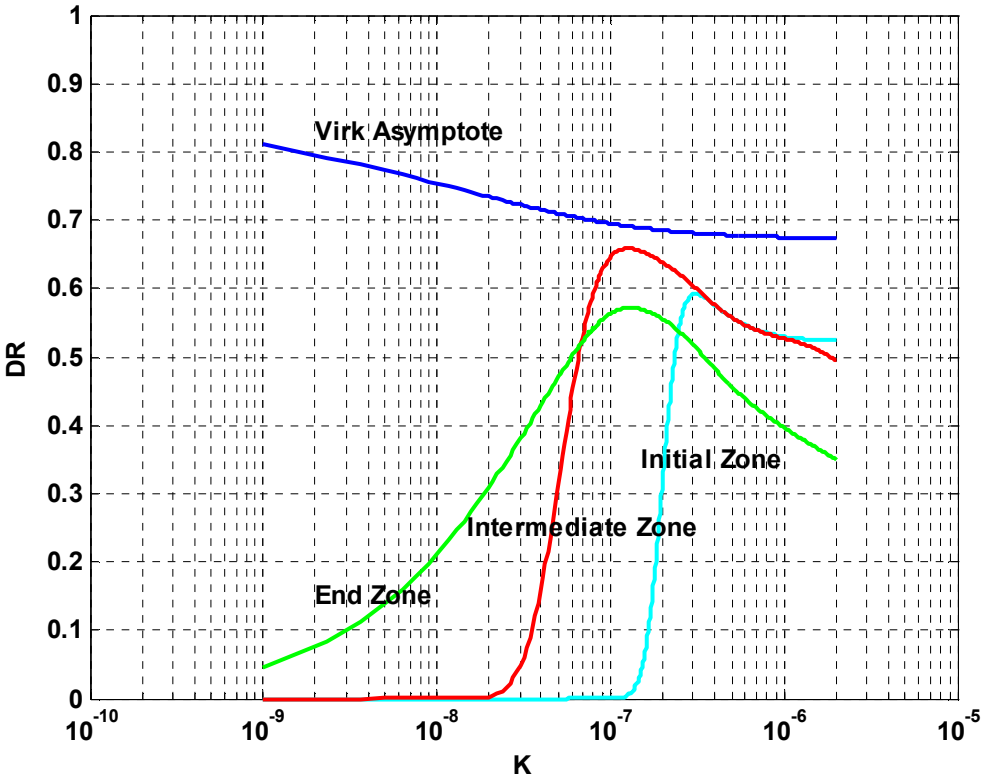

Figure 5: Components of total friction reduction

Figure 6 shows the total concentration at the wall as a function of K and compares the total with the model results for the three zones. For this example, the cross-over point between the intermediate zone and the far zone at K ~ 6.5 10^{-8} is obvious. The cross-over point between the initial zone and the intermediate zone occurs around K ~ 4.5 10^{-7}.

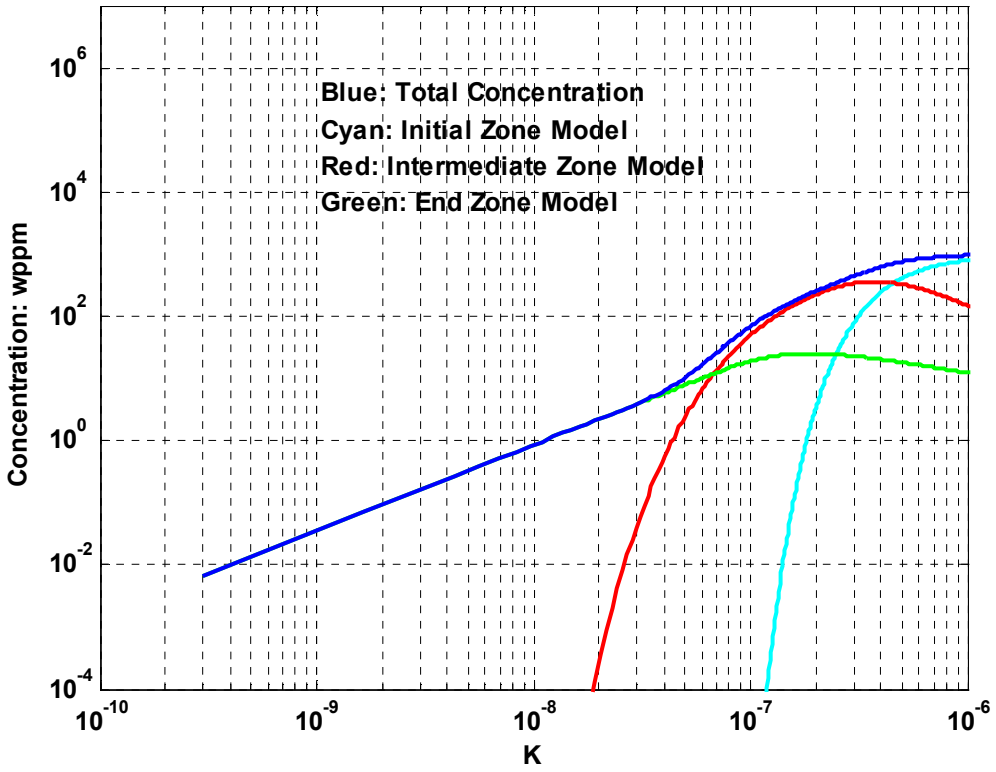

Figure 6: Components of wall concentration

The following sections examine the sensitivity of the model to each of the parameters.

5.1.1 Sensitivity to k_0

The k_0 parameter was introduced by Vdovin & Smol'yakov to compare the performance of different polymer types. By definition $k_0 = 1$ refers to PEO WSR-301. Any polymer with poorer performance will have a value of $k_0 < 1$. Any polymer with superior performance will have a value of $k_0 > 1$. Note that Vdovin & Smol'yakov relate this standard value to 'fresh' polymer, and they provide data that indicate that 'aged' WSR-301 can have a k_0 value of ~0.2. As Figure 7 shows, performance of the model is sensitive to k_0. The general effect is to shift the curves left or right without significant change of shape.

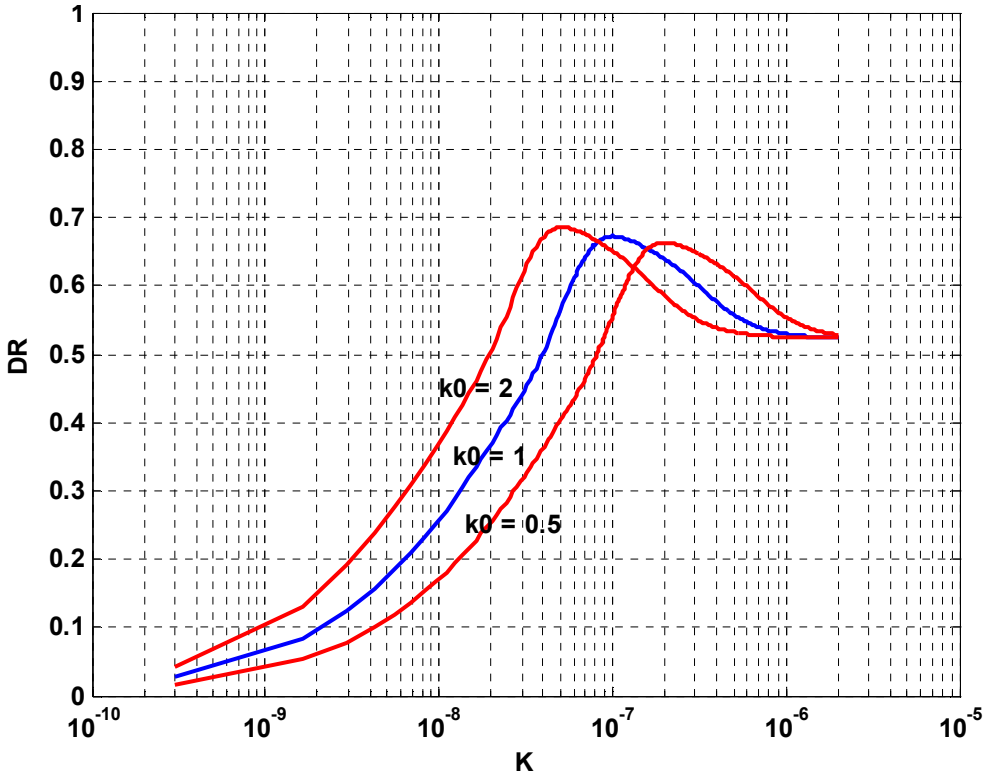

Figure 7: Sensitivity to k_0

5.1.2 Sensitivity to L_{max}

The parameter L_{max} was introduced to account for the possibility that the diffusion length, L, saturates or reaches an asymptotic value as other experimental parameters change. As Vdovin & Smol'yakov showed, $L_{max} \sim 70$ cm when the ejection angle is small. However, when the ejection angle was large, they did not find any limiting behavior of L. Figure 8 shows that the model behavior is not sensitive to L_{max} unless L_{max} assumes unrealistically small values. In practical terms, this implies that

$$x_s/L \approx 1/kK \tag{39}$$

almost everywhere without the need for the correction factor F of Equation (37).

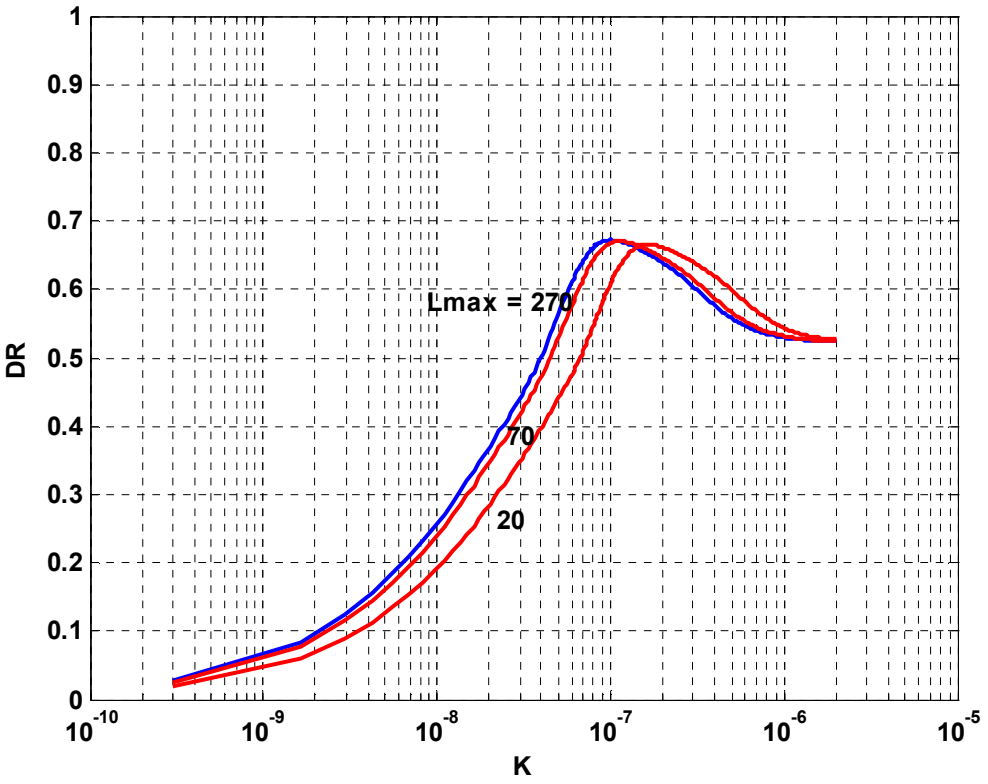

Figure 8: Sensitivity to L_{max}

5.1.3 Sensitivity to U_{ref}

U_{ref} is a parameter taken directly from Petrie *et al*, and there is no reason to assume that it is in error. As Figure 9 shows, the model is not sensitive to 25% - 35% errors in U_{ref}. The only effect is a slight shift of the curves left or right without change of shape. Thus the nominal value of this parameter appears to be adequate for the model.

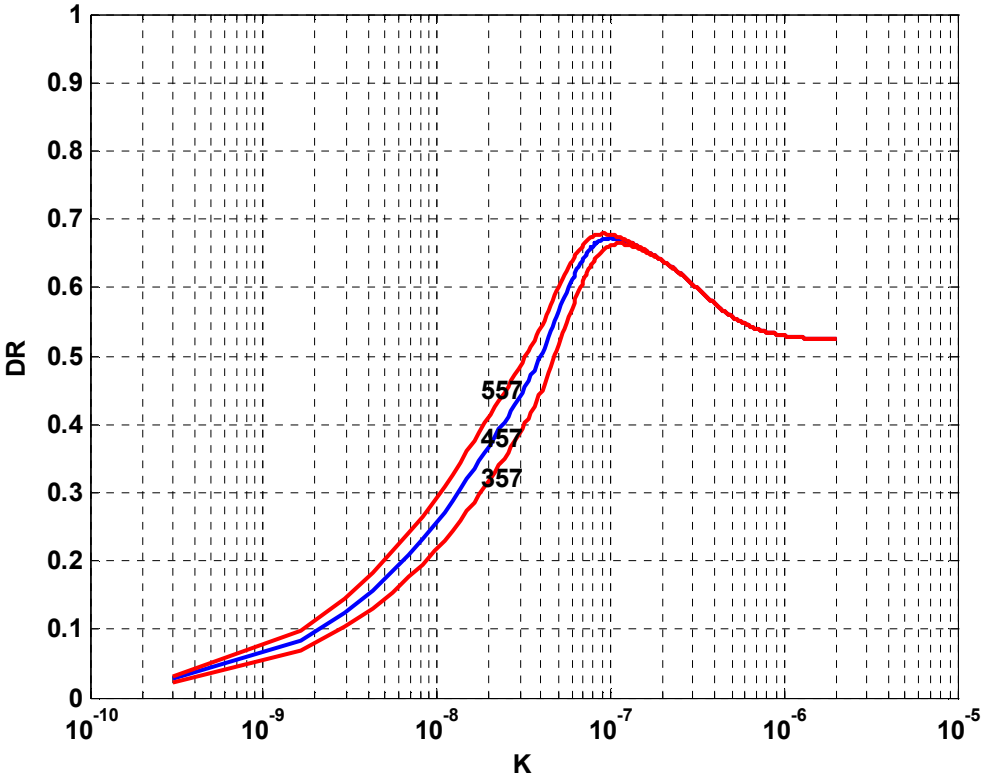

Figure 9: Sensitivity to U_{ref}

5.1.4 Sensitivity to γ

The parameter γ, which appears in the exponent that governs the approach to saturation as a function of wall concentration, has a modest influence of the model. In general, increasing γ increases the apparent performance of the polymer. As Figure 10 shows, changes in γ cause a shift of the whole curve left or right without significant change of shape.

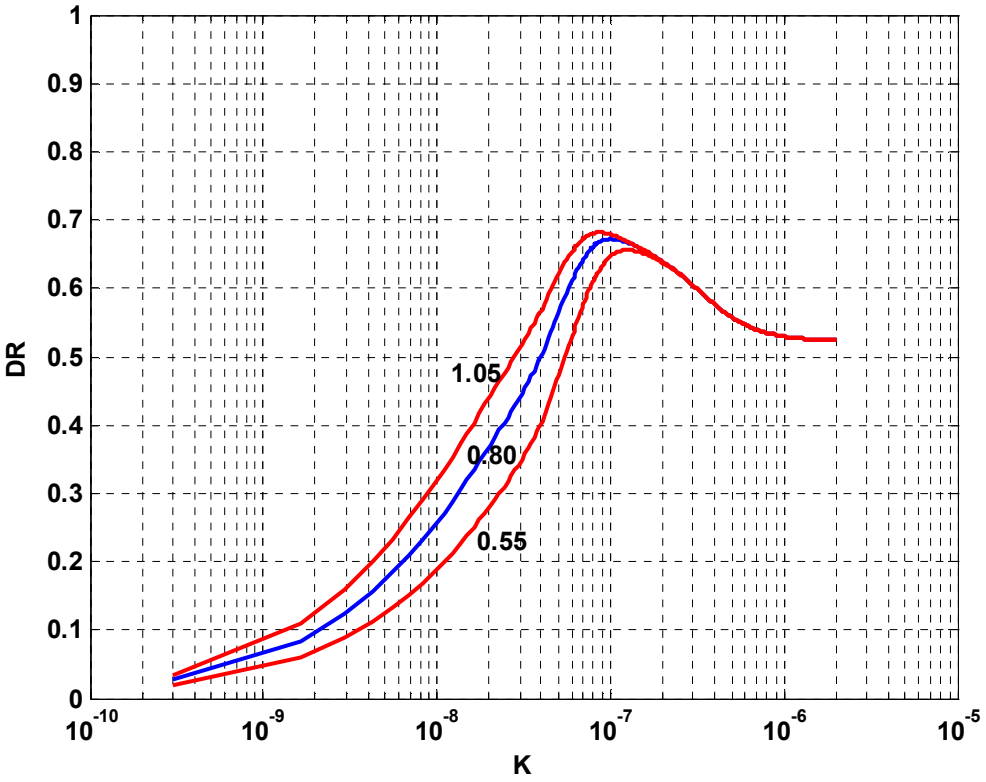

Figure 10: Sensitivity to Gamma (γ)

5.1.5 Sensitivity to δ

The parameter δ is the power law exponent that describes the contribution of the velocity in the approach to saturation as a function of wall concentration. Figure 11 shows that the model is not sensitive to changes of δ within a reasonable range around its nominal value.

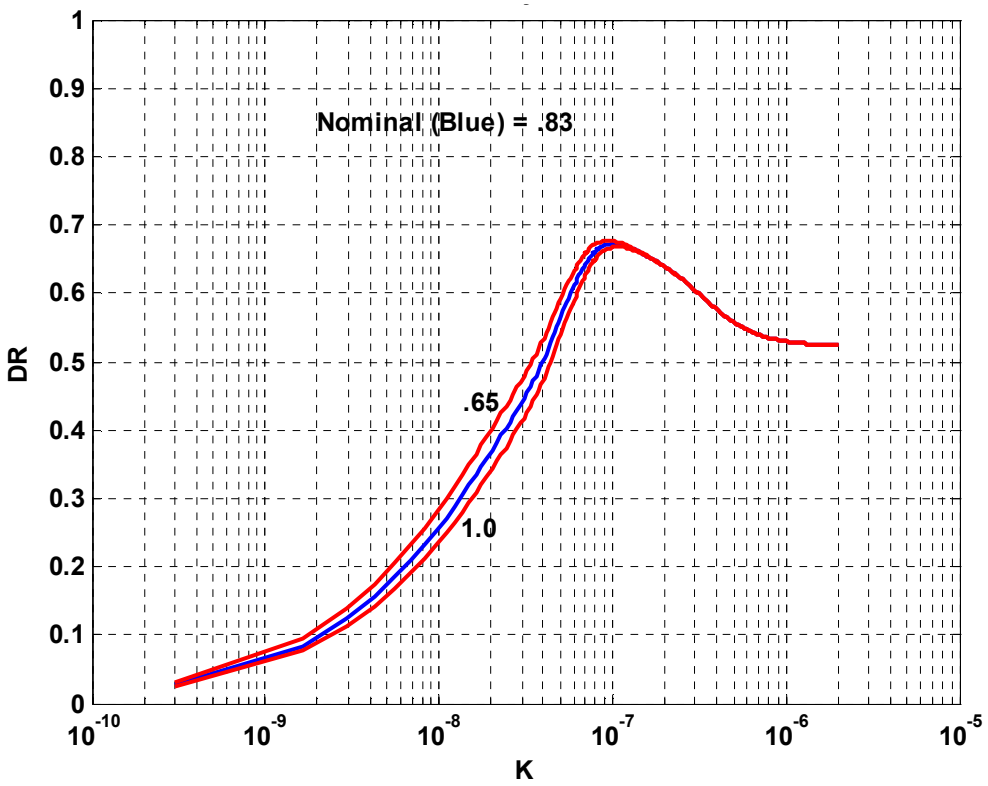

Figure 11: Sensitivity to Delta (δ)

5.1.6 Sensitivity to ββ

The parameter ββ is the power law exponent of the concentration in the approach to saturation from below. Figure 12 shows that this parameter has a major impact on the magnitude and shape of the DR vs. K curve. In particular, it changes the slope of the curve in the diffusion far zone. This parameter provides a sensitive test of the correctness of the model. It is thus very important to have a reliable estimate of the value of ββ from independent sources. The data of Petrie *et al* from polymer ocean experiments is limited in scope and accuracy. Examination of additional data from other polymer ocean experiments and from pipe experiments should improve the estimate of ββ.

At a deeper level, it will also be important to understand why this scaling parameter is approximately 1/2, and to justify the assumption that the scaling approach to saturation observed in polymer ocean and pipe experiments also applies to external flow conditions.

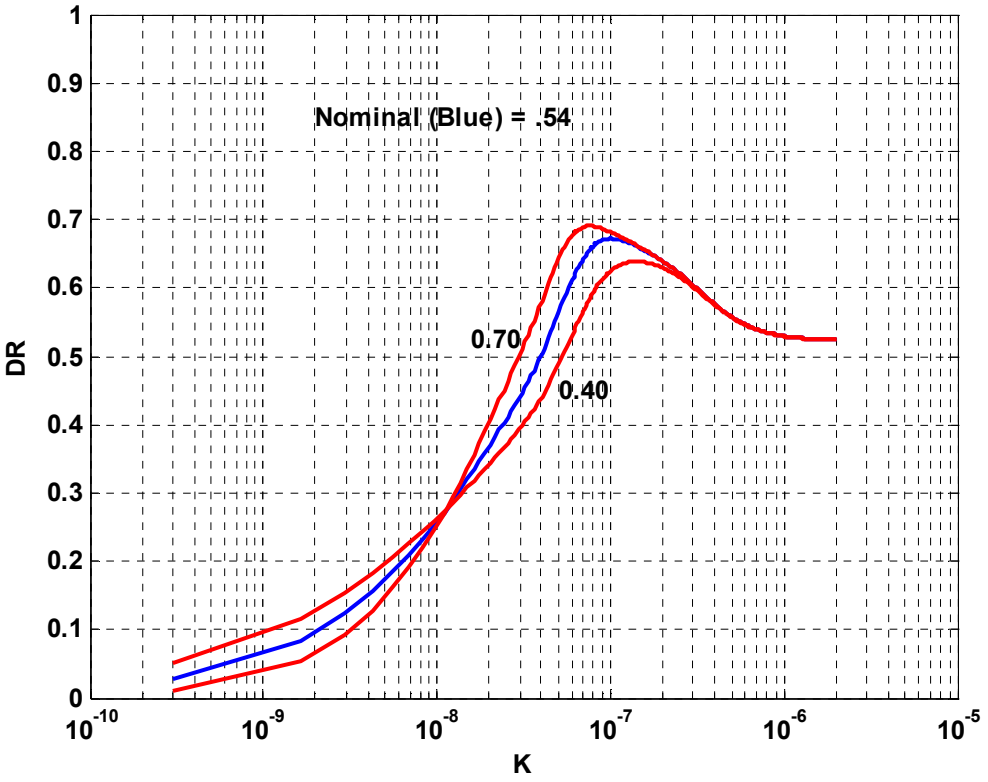

Figure 12: Sensitivity to Double Beta (ββ)

5.1.7 Sensitivity to c_{roll}

The value of the roll-off parameter for high-concentration effects, c_{roll}, has a significant impact on the model in the near-slot region where the initial polymer concentration is high, refer to Figure 13.

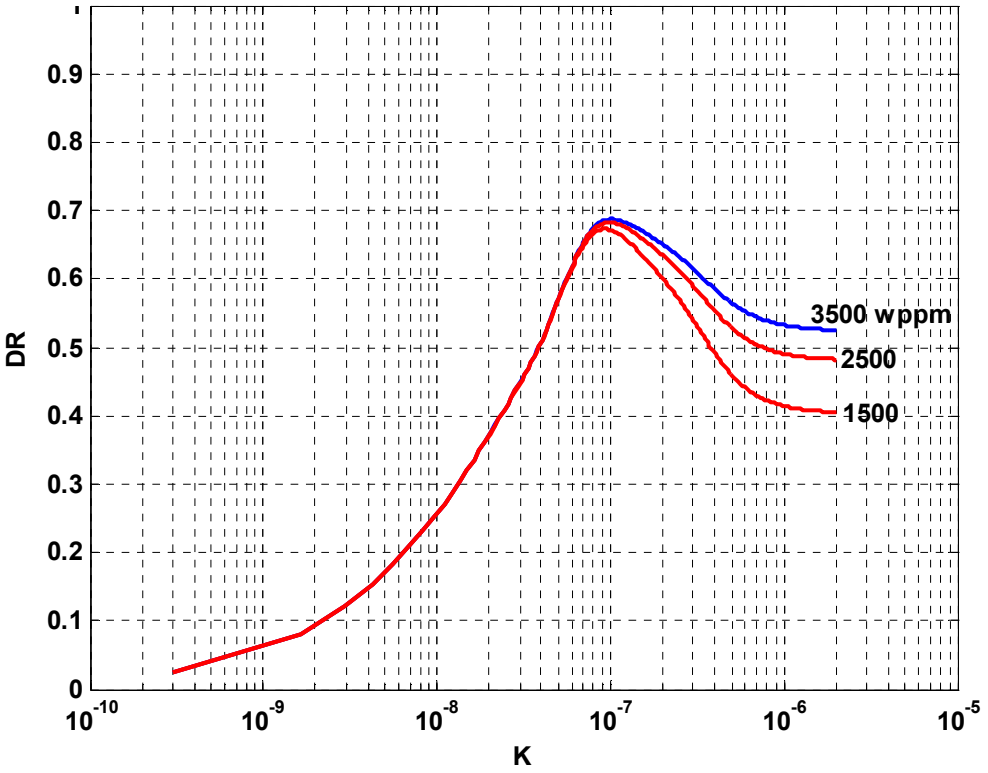

Figure 13: Sensitivity to c_{roll} (wppm)

5.2 *Influence of Experimental Conditions*

Polymer friction reduction experiments have been conducted on the external surface of flat plates, bodies of revolution, and operational marine vehicles. For purposes of comparing experimental conditions, the flat plat provides the simplest example. The principal parameters that can be varied in the course of an experimental investigation are: U_∞, the free stream velocity; x_0, the longitudinal coordinate of the slot with respect to the virtual origin of the turbulent boundary layer; the slot ejection angle, ϕ, manifest through the angle parameter, α; the initial concentration of ejected polymer, c_0; and the polymer ejection rate, q.

The influences of these experimental parameters on the model are discussed next. As in Section 5.1, the set of nominal empirical parameters and the set of nominal operating conditions provide the baseline case. The effects of the experimental parameters are demonstrated by varying them, one by one, from their nominal values.

5.2.1 Influence of Free Stream Velocity

The influence of free stream velocity is shown in Figure 14. Two separate effects are apparent.

In the diffusion far zone region, there is a significant separation between performance curves at different values of U_∞. Superior performance is predicted by the model at smaller values of U_∞. That separation is a consequence of the scaling of the approach to saturation, $(U_{ref}/U_\infty)^\delta$. The fact that both U_∞ and c obey power laws *with different exponents* ensures that the ratio c/U_∞ does not collapse to a common curve.

In the region controlled by Virk's asymptote, the order is reversed, and superior performance is attained at higher values of U_∞. That is because the maximum friction reduction predicted by Virk's asymptote is an increasing function of Reynolds number, hence of U_∞.

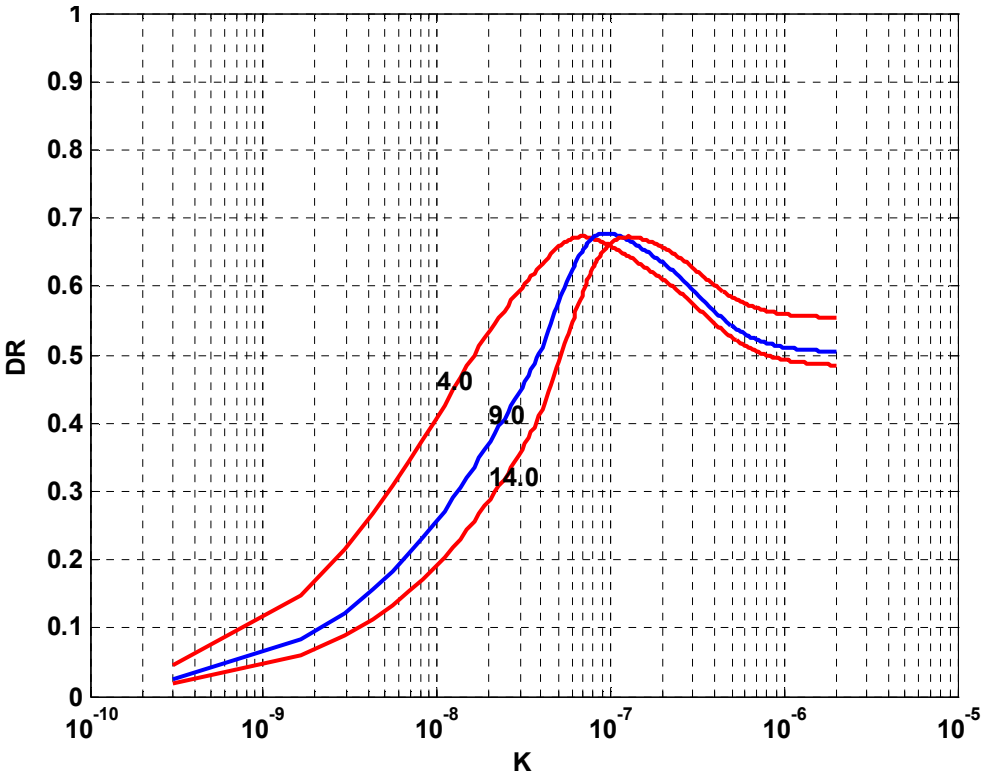

Figure 14: Variation with free stream velocity (m/s)

5.2.2 Influence of Slot Position re Virtual Origin

The parameter x_0 only influences friction reduction performance in the region controlled by Virk's asymptote. This is also a consequence of the dependence of the asymptote on Reynolds number. For a given value of K, the operative Reynolds number in the

calculation of the maximum friction reduction, Re_x, is increased by the Reynolds number Re_{x0}, which is a linear function of x_0. Thus, as x_0 increases (greater separation between the virtual origin and the slot position), the maximum friction reduction also increases, as illustrated in Figure 15.

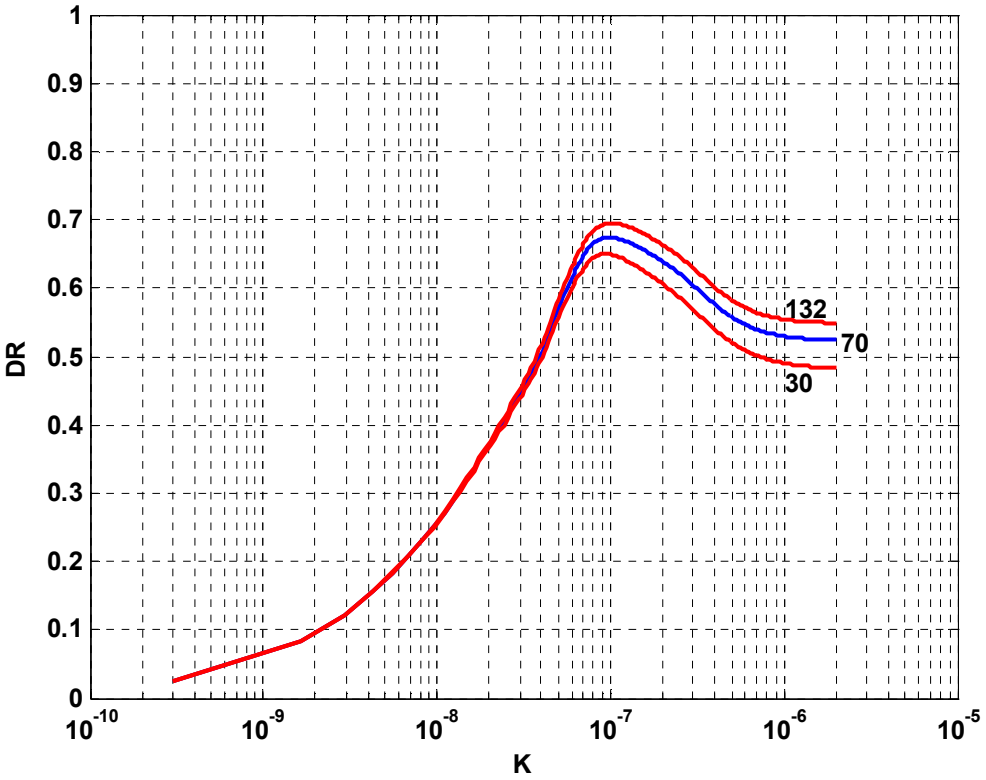

Figure 15: Variation with Slot Position x_0 (cm)

5.2.3 Influence of Slot Angle Parameter α

The model does not yet contain a relationship between the ejection angle and the parameter α. Vdovin & Smol'yakov only report results for two ejection angles. Their results show that α is an increasing function of ϕ. Values of α for ejection angles greater than their maximum angle of 20° must be extrapolated.

Sensitivity studies with the present model show that the predicted performance of the polymer depends very strongly on α. For that reason, accurate knowledge of α over a realistic range of ejection angles, as well as a fundamental understanding of the physics of varying ejection angles, becomes very important.

Figure 16 shows that small values of α extend the intermediate diffusion zone to significantly smaller values of K. Part of that extended range is controlled by Virk's asymptote, allowing high friction reduction and superior performance over a greater distance downstream of the slot. Where the performance is controlled by the exponential

damping function of the intermediate zone, the slope of the performance curve is very steep. For smaller values of K, the high-slope intermediate zone blends into the gentler algebraic slope of the far zone.

The model implies that smaller ejection angles and smaller α values would show superior performance over an even wider region of K space.

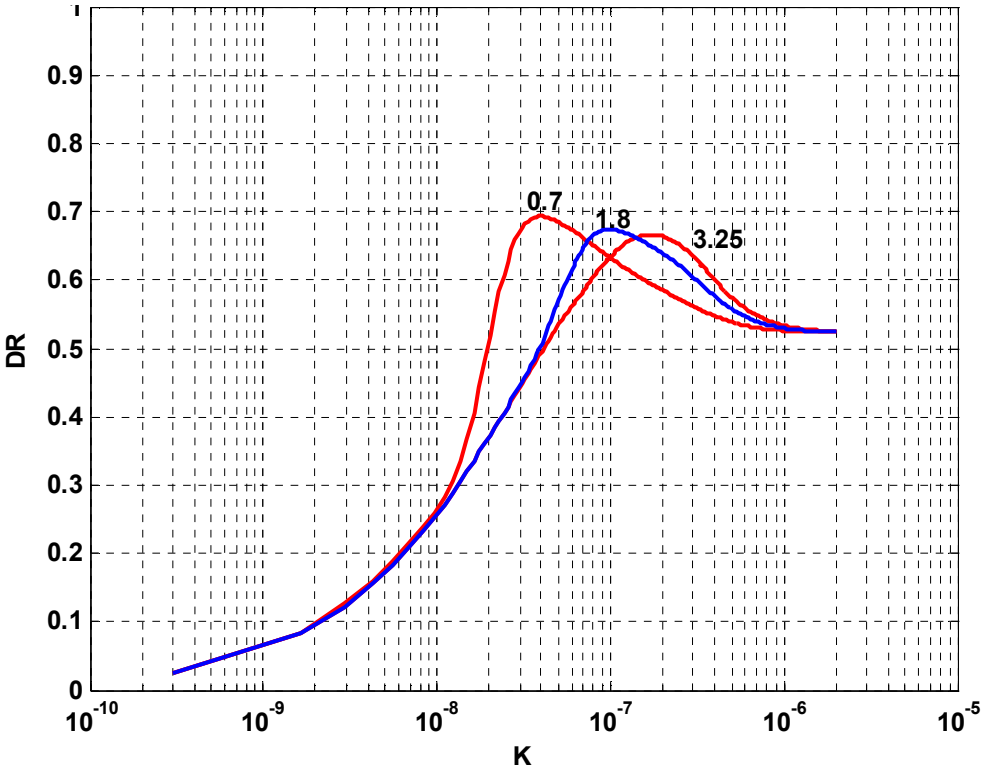

Figure 16: Variation with Slot Angle Parameter Alpha (α)

5.2.4 Influence of Initial Concentration c_0

According to the results of Vdovin and Smol'yakov, the wall concentration is explicitly proportional to the initial concentration in the initial and intermediate zones, but not in the far zone. That dependence of their model is reflected in Figure 17, which shows significant dependence of performance on c_0 in the intermediate zone. The dependence essentially vanishes in the far zone, where any dependence on c_0 is implicitly contained in L. But the strongest dependence on c_0 occurs in the initial zone, where the effects of entanglement become manifest for large values of concentration. The dependence on c_0 is also impacted by the choice of c_{roll}. In the example shown, $c_{roll} = 3500$ wppm. This causes a large decrease in friction reduction when $c_0 = 4000 > c_{roll}$, but produces no obvious effect when $c_0 = 100 << c_{roll}$.

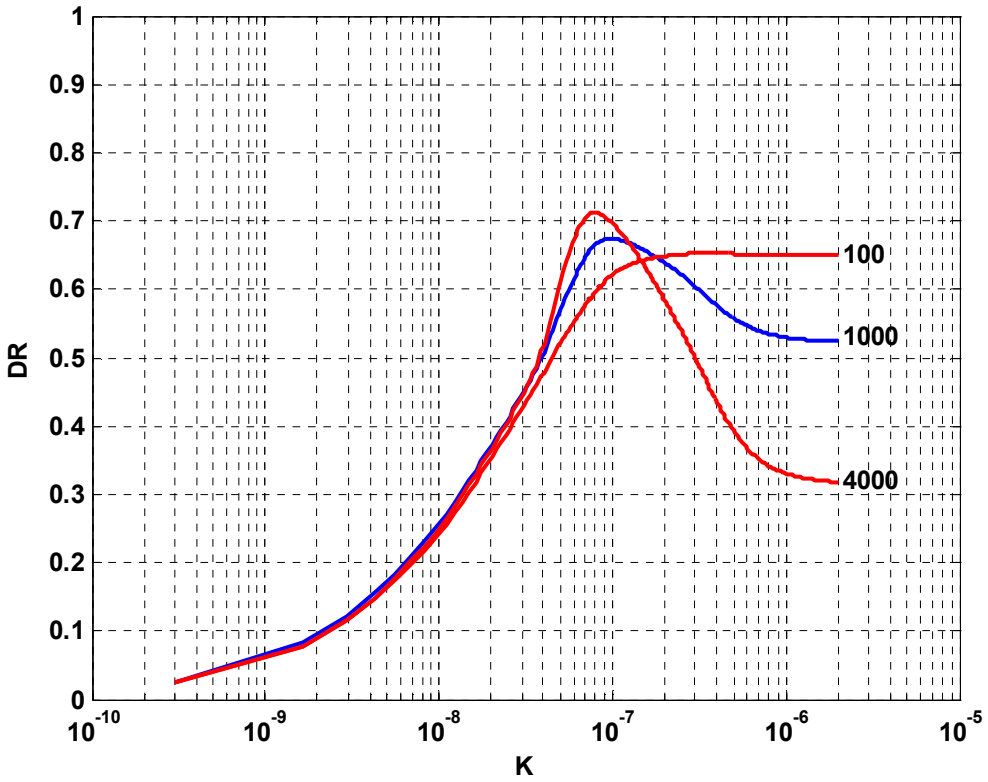

Figure 17: Variation with Initial Polymer Concentration c_0 (wppm)

5.2.5 Influence of Polymer Ejection Rate q

In the same spirit, the friction reduction performance depends weakly on the ejection rate, q, only in the initial and intermediate zones. Figure 18 shows that ejection rate does not influence performance in the far zone. In that zone the K factor collapses the q dependence to a single line that incorporates the product $qc_0/\rho x$, but, as shown in Section 5.2.1, does not properly collapse with $1/U_\infty$. As discussed in Section 7 below, q is determined by the ejection velocity and the slot width.

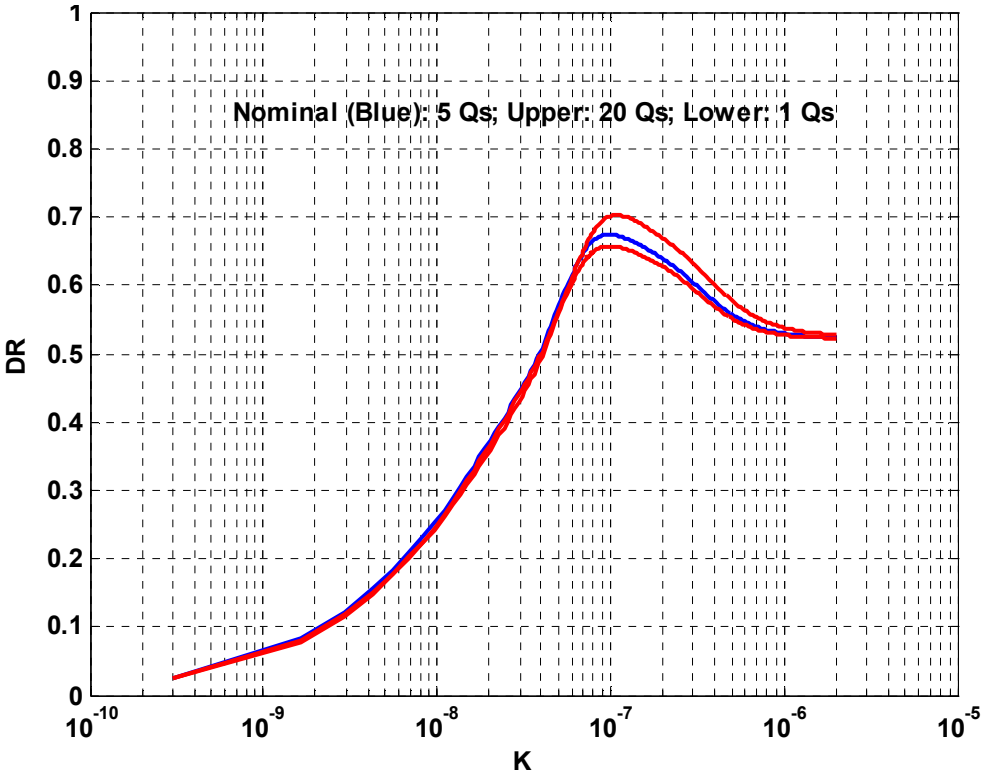

Figure 18: Variation with Polymer Ejection Rate (q)

6 Comparison with Published Experiments

In this section, the model is exercised to compare its predictions with data published by various experimental groups. These data are independent of the data used to build the model. Consequently, these comparisons should provide a good test of the model.

6.1 *Data of Winkel et al (2006)*

Recent experiments were reported by Winkel *et al* (2006). Their results are of particular interest because they show a strong effect of free stream velocity. Data taken at different values of U_∞ do not collapse onto a single curve in the DR vs. K plot.

The experiments were conducted in the William B. Morgan Large Cavitation Channel in Memphis, TN. Experimental conditions were as follows.

Polymer type:

PEO WSR-301, WSR-N-60K, WSR-308

Slot Position re Leading Edge:

x_0: 132 centimeters

Drag Measurements re Slot Position:

x_s: -25, 64, 209, 611, 791, 1018 centimeters

Free Stream Velocity:

U_∞: 600, 1200, 1800 centimeters/second

Polymer Concentration:

c_0: 1000, 2000, 4000 wppm

Ejection Rate:

q: 2Qs, 4Qs, 10Qs

Ejection Angle:

$\phi = 25^\circ$.

Extensive amounts of data were collected, and several of the data sets were presented in the DR vs. K format. Of particular interest are (1) comparisons among different free

stream velocities for PEO WSR-301 (Winkel *et al*'s Figure 16, reproduced here as Figure 19), and, (2) comparisons among different polymer types for various free stream velocities.

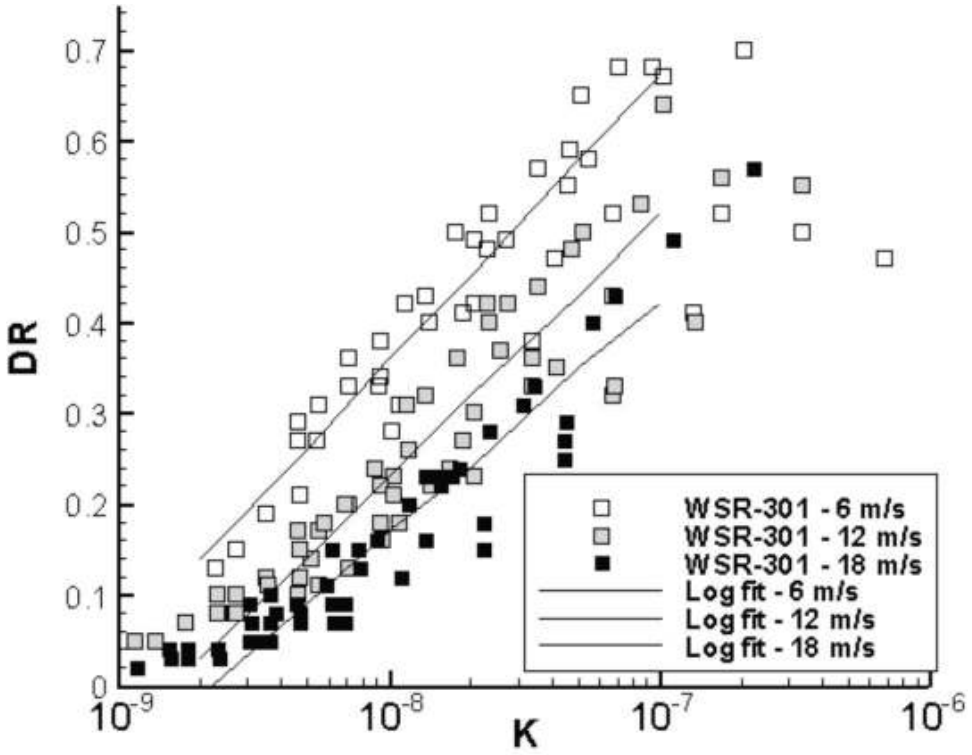

Figure 19: [from Winkel, et al., *Proc. 26th Symposium on Naval Hydrodynamics*, (2006)]

To make comparisons with the published data, the model was exercised with the nominal empirical parameters. Those parameters were then adjusted to provide the best fit to the data of Winkel *et al*. Large adjustments were found to be unnecessary. All of the experimental parameters were specified except α. The largest ejection angle tested by Vdovin & Smol'yakov was 20°, corresponding to $\alpha = 1.8$. In the present case, the α value was extrapolated to ~25° by scaling according to sine(ϕ), giving $\alpha \approx 2.25$. At present the sine(ϕ) scaling is a heuristic without a rigorous basis in theory.

Figure 20 compares the output of the model with the data of Winkel *et al*. for three different free stream velocities. The match appears to be good. DR values at K values $K = 10^{-8}$ and $K = 10^{-7}$ are accurate for each free stream velocity. The irregular spacing between the different velocity curves is also accurately predicted. The decreased performance due to high concentrations in the near-slot region (initial zone) is also predicted.

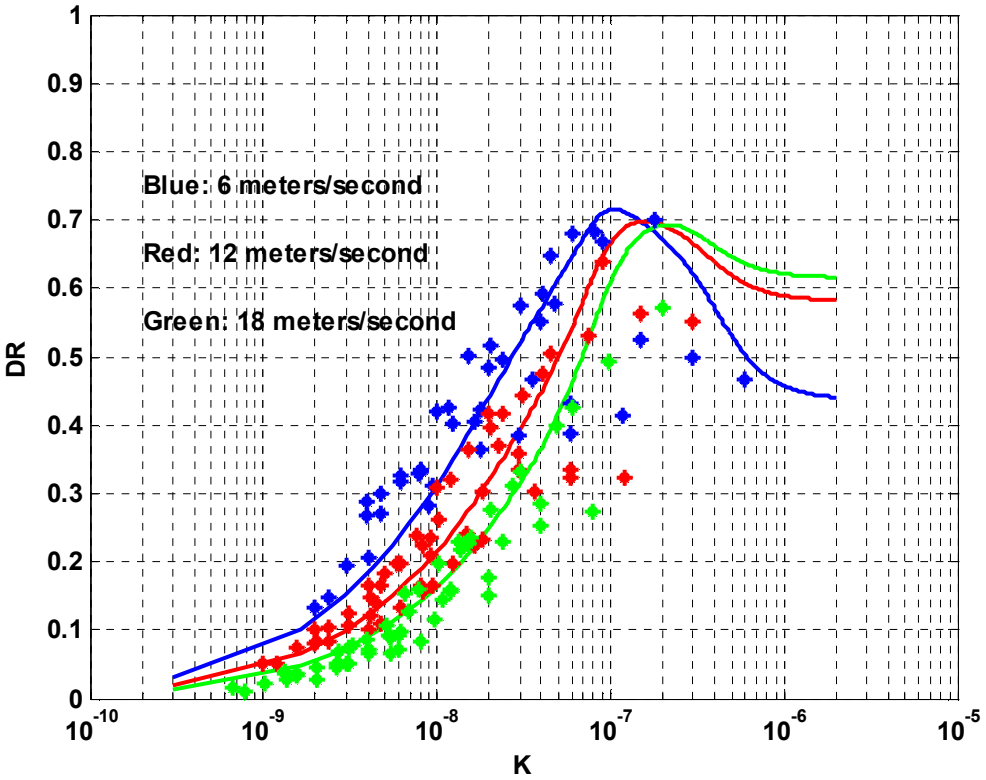

Figure 20: Comparison of Model with Data of Winkel, et al.

Differences in polymer type are expressed through the empirical parameter k_0 of Vdovin & Smol'yakov. The reference value is $k_0 = 1$ for WSR-301. Based on pipe flow data, WSR-308 has a value $k_0 \approx 2$. The value for WSR N60-K is not known. A value $k_0 = 0.2$ was used to give a reasonable match to the data of Winkel *et al*.

Figure 22 shows the model output for the three polymer types at $U_\infty = 6$ m/s. The curves for 301 and 308 accurately reflect the data in Winkel *et al* [Winkel *et al*'s Figure 15(A) reproduced here as Figure 21] without any parameter adjustment. The curve for N60-K accurately matches the data after assignment of $k_0 = 0.2$ to that polymer.

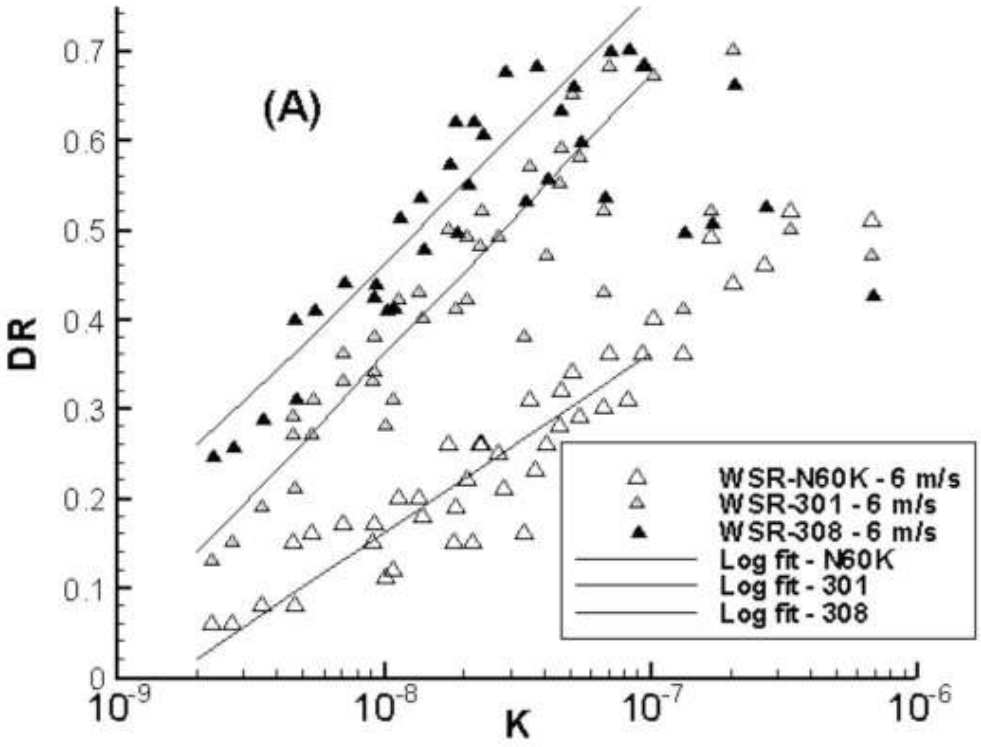

Figure 21: [from Winkel, et al., *Proc. 26th Symposium on Naval Hydrodynamics*, (2006)]

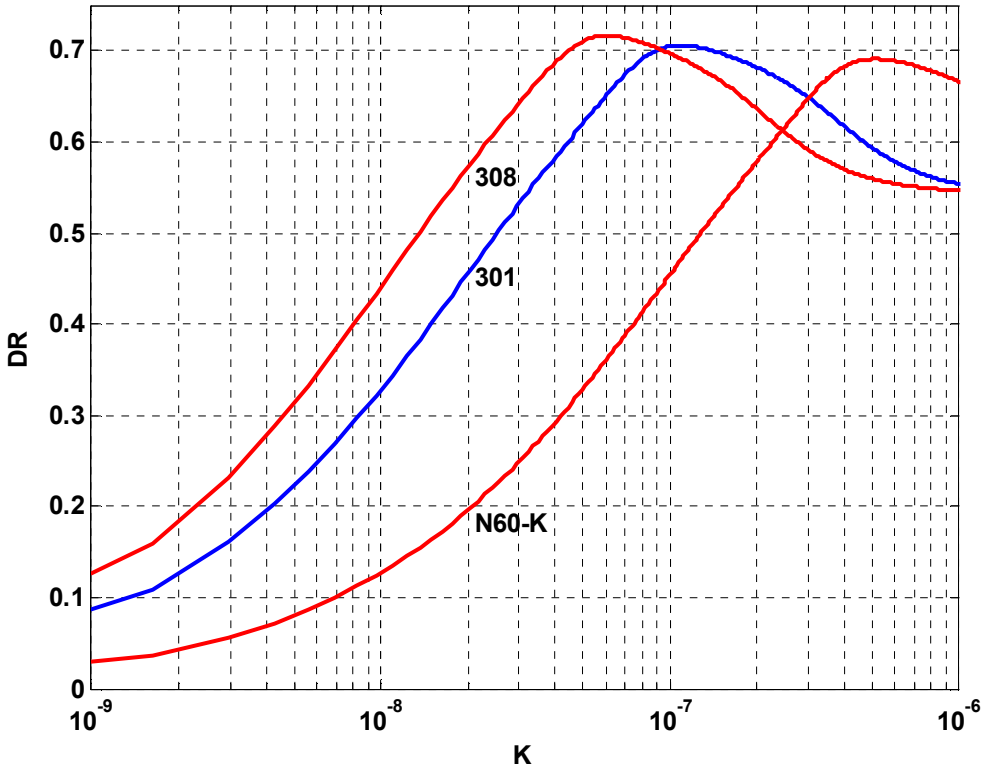

Figure 22: Variation with Polymer Type: 6 m/s

6.2 *Data of Cortana Corporation*

Experiments were conducted at the Applied Research Laboratories of Pennsylvania State University, using an ejection slot designed by Cortana Corporation.

Experimental conditions were as follows.

Polymer Type:

PEO WSR 301; WSR 309

Slot Position re Virtual Origin (Tripped BL):

x_0: 27.9 centimeters

Drag Measurements re Slot Position:

x_s: 7.7, 200, 329, 474, 646 centimeters

Free Stream Velocity:

U_∞: 457, 762, 1067 centimeters/second

Polymer Concentration:

c_0: 500, 1000, 2000 wppm

Ejection Rate:

q: 5Qs, 10Qs, 20Qs

Ejection Angle:

$\phi = < 5^\circ$.

Comparisons between measurements and model predictions are shown in Figure 23, where the model is modified to adhere to the observation of Vdovin & Smol'yakov that: *for small ejection angles, the behavior of the polymer is governed by inner variables alone, not by outer variables such as* U_∞. That is, in the intermediate and far zones, the data collapse to a single function of K, *independent of free stream velocity*.

An important feature of this case is the effect of the small slot angle. The use of a small value for the α parameter extends the impact of the intermediate zone toward smaller K values and predicts a steeper slope in the region $10^{-8} < K < 4 \times 10^{-8}$. Those predictions match the ARL/Cortana experimental data very well. Comparison with the data of Winkel *et al* (Figure 20) shows that their large slot angle (25°) minimizes the role of the

intermediate zone; their shallower slope in the region $10^{-8} < K < 10^{-7}$ indicates behavior characteristic of the far zone over most of their measurement range.

The Cortana data exhibits large variability in the initial zone, that is, in the near-slot region ($K > 2 \times 10^{-7}$), including some performance that exceeds the predicted Virk asymptote. A separate analysis in the following section indicates that the ejection velocity (related to q and slot width) has a significant impact in the near-slot region.

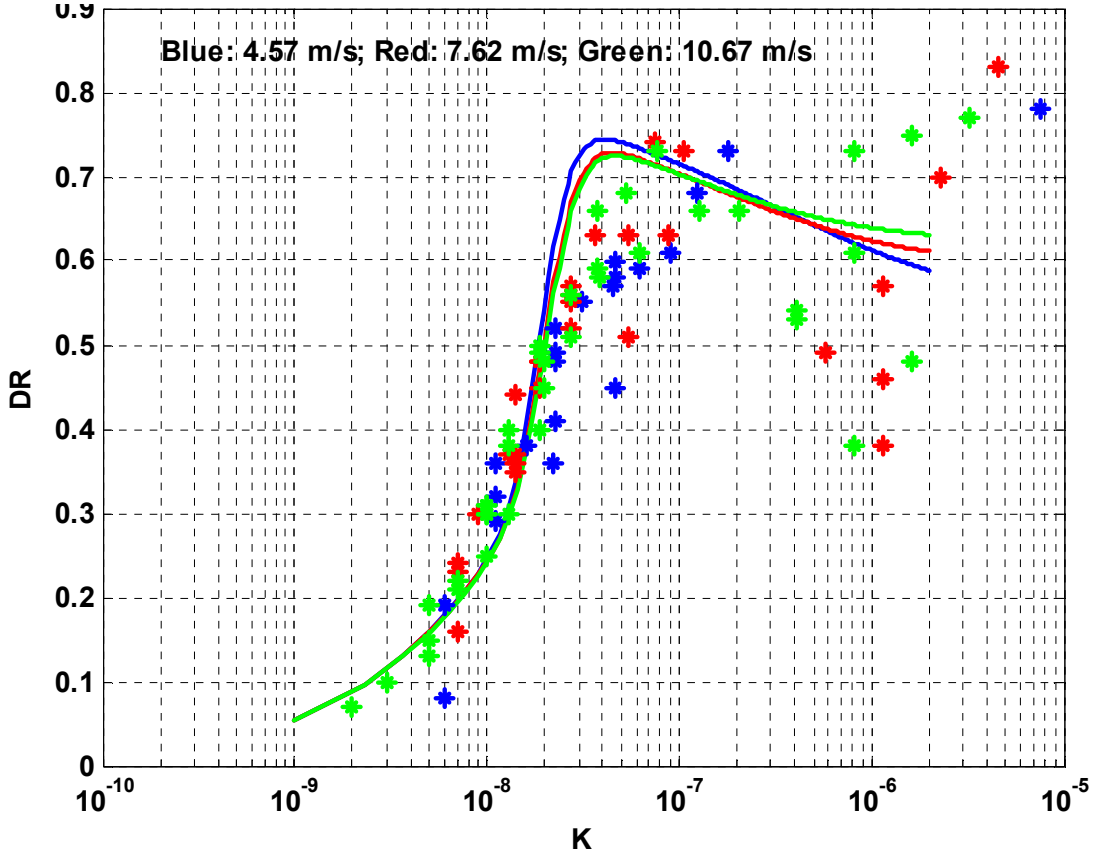

Figure 23: WSR 301 Cortana Fluidics Ejector; Model: Inner Variable Hypothesis

7 Near-Slot Effects

Discrepancies between the model and the Cortana data tend to be largest for large values of K. Those K values correspond to small values of x, very close to the injection slot. In that region, there is a large amount of scatter in the friction reduction performance; however, the scatter is not totally random, and appears to be correlated with q and c_0, variables that are related to the properties of the polymer at the point of ejection.

In the Cortana WSR 301 data taken on the GTV by ARL/PSU, there were 14 data sets for measurements at a location 7.7 centimeters from the slot. Friction reduction varied from .38 to .83, from well below to slightly above Virk's asymptote for that location and Reynolds number. The free stream velocity did not appear to have any significant influence on the friction reduction for these data sets. The ejection rate q had a strong positive influence, and the initial concentration of polymer, c_0, had a weak and statistically insignificant influence on friction reduction.

A linear regression model of DR vs q/Qs and c_0 in the near-slot region produced a fit that accounted for 66% of the variance:

$$DR = .2826 + .0194\ q/Qs + .000039\ c_0. \qquad (40)$$

q/Qs alone accounted for 63% of the variance. These calculations show that q/Qs plays a dominant role in the friction reduction performance of polymer solutions near the ejection slot, and raise an important question about the physical mechanism behind this behavior.

At present an accurate quantitative model of the near-slot environment is not yet available. Nonetheless, there are enough observations in the literature to support qualitative arguments and to build an approximate model.

First, it is widely accepted that enhanced drag-reduction performance of a polymer solution is observed when the individual polymer molecules are in the extended configuration, rather than in the coiled configuration. Thus, the coil-stretch transition is an important marker of friction reduction performance.

Quantitative description of this transition typically uses a two-state model: transition from the coiled configuration to the stretched configuration is caused by elongational forces in the fluid flow; reversion to the coiled state is caused by elastic forces of the molecule itself when the extensional fluid forces are temporarily reduced. The quasi-equilibrium condition of a polymer molecule in a particular flow is determined by the relative time scales on which these competing processes operate. An extended polymer molecule relaxes on multiple time scales, but the governing effect is that of the longest molecular relaxation time, τ_{max}. The fluid time scale is estimated as the reciprocal of the strain rate of the elongational flow $[dU/dx]^{-1}$. The ratio of these time scales is called the Weissenberg number, Wi, and is used as a measure of the state of the polymer with

respect to the coil-stretch transition. Often the elongational time scale is not easily determined, and the shear time scale $[dU/dy]^{-1}$ is used as a proxy.

For much of the history of polymer research, only bulk properties could be measured, and the behavior of polymers as a function of Weissenberg number was not accurately known. Wi ~ 1 was taken as an approximate indicator of the coil-stretch transition. Beginning in 1994, techniques for single-molecule observations and quantitative measurements were developed. These led to a much better understanding of the dynamics of single molecules, and to an appreciation of the effects of different types of flows on the coil-stretch transition. Key papers in this body of research include Perkins *et al*, 1994a, Perkins *et al*, 1994b, Perkins *et al*, 1995, Larson *et al*, 1997, Perkins *et al*, 1997, Smith & Chu, 1998, Smith *et al*, 1999, Dua & Cherayil, 2000a, Dua & Cherayil, 2000b, Hur *et al*, 2002, Dua & Cherayil, 2003, and Schroeder *et al*, 2003.

Most pertinent to the present discussion are the papers of Perkins *et al*, 1997 and Smith *et al*, 1999. Comparison between those two papers shows that there is a very significant difference between elongational flow and shear flow. In elongational flow, the mean fractional extension of the polymer molecule increases very rapidly with Weissenberg number, reaching ~80% mean fractional extension for Wi ~ 5, then slowly approaching ~95% for Wi ~ 50. In shear flow, the mean fractional extension grows much more slowly with Wi and reaches an asymptotic value of only ~ 50% for large Wi. Figure 24 below, taken from Smith *et al,* illustrates the aforementioned point.

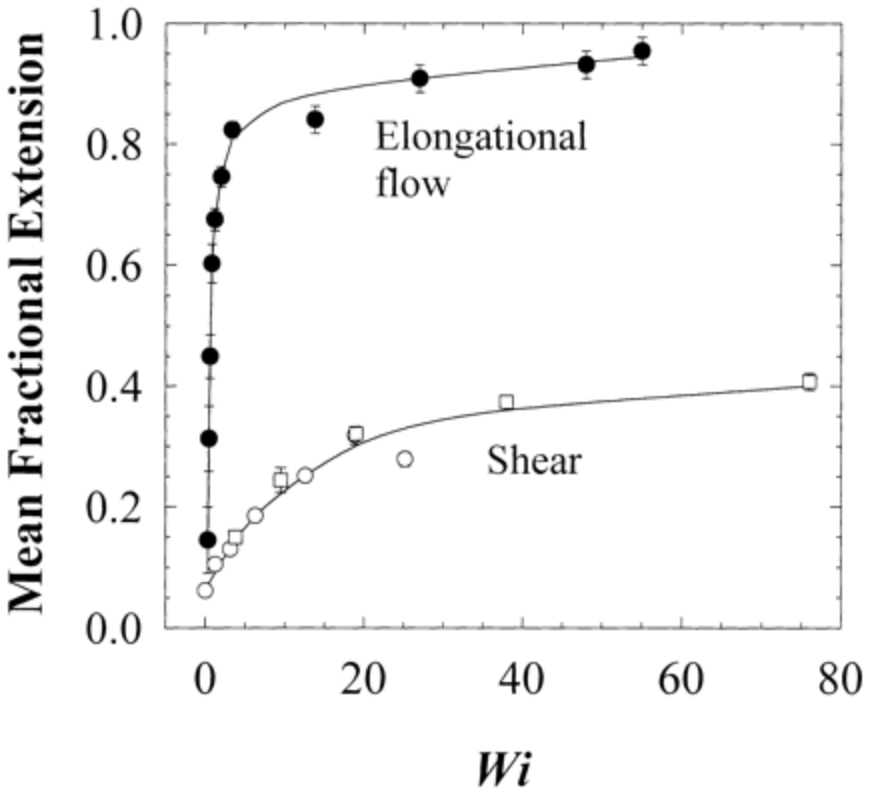

Figure 24: [from Smith, et al., *Science* 283, 1724-1727, (1999)]

The relevance of these observations for slot-ejected polymer friction reduction can be profound. A well-designed ejection slot should produce primarily elongational flow, in which the polymer is efficiently extended and preconditioned for friction reduction before it enters the external flow. Such preconditioned molecules can be effective immediately. On the other hand, if the ejection slot does not produce elongational flow, a significant fraction of the polymer will enter the turbulent boundary layer of the external flow in the coiled configuration. As Smith *et al* showed, the shear flow of the boundary layer is much less efficient at uncoiling the polymer molecules, and significant delays may ensue before friction reduction reaches its full potential (as measured by Virk's asymptote.)

A second point may also be relevant. Virk's asymptote was originally derived from empirical observations of turbulent shear flow in pipes, and has since been generalized to turbulent shear flows in other configurations. It represents the optimum friction reduction performance that can be achieved in shear flow with a mean fractional extension of ~50%. When the mean fractional extension of the polymer molecules approaches 90%, as in extensional flow at large Weissenberg numbers, the friction reduction performance may exceed that predicted by Virk's asymptote, and may be described by a separate asymptote. The nature of that separate asymptote is yet to be defined, but one can conjecture that it depends on the Weissenberg number and possibly on the Reynolds number as well.

A preconditioned polymer solution leaving the elongational flow environment of the ejection slot will soon interact with the turbulent external flow. As a result of mixing with the dominant external flow, the mean fractional extension of the polymers will relax toward 50%, consistent with shear flow conditions. The relaxation time for this process is likely to be significantly longer than the relaxation time for a single molecule (typically ~ 3 milliseconds), but the exact value is not known. The relaxation time may also depend on the ejection angle of the slot, which would influence the amount of time spent in the viscous sublayer before entering the turbulent shear flow outside the viscous sublayer.

The Weissenberg number for the ejection flow is directly proportional to q. Consequently, the mean fractional extension of the ensemble of polymer molecules is an increasing non-linear function of q, consistent with Figure 24. To illustrate this point, in a simple model of a linearly converging channel with half-angle α and exit width w_s, the maximum rate of strain at the exit is

$$dU/dx_{max} = 2 \tan(\alpha)\, u_{ej}/w_s, \qquad (41)$$

and, since

$$q = n\, Qs = u_{ej}\, w_s, \qquad (42)$$

the Weissenberg number is

$$Wi = \tau_{max} (2 \tan(\alpha)/w_s^2)q. \qquad (43)$$

Other channel geometries would preserve the linear relationship between q and Wi, albeit with different proportionality factors.

These considerations suggest the outlines of an approximate model postulated to account for the near-slot behavior observed in the Cortana data.

- For elongational flow there exists a friction reduction asymptote that exceeds the Virk asymptote for shear flow. The maximum friction reduction values for elongational flow are presently unknown, but are expected to be a non-linear function of the Weissenberg number, hence of the ejection flow rate.

- For large values of the ejection flow rate, local friction reduction near the slot is expected to attain this new asymptote almost immediately.

- After a finite period of mixing with the external flow, the behavior of the polymer relaxes from the new asymptote toward the Virk asymptote for shear flow. The relaxation time is equivalent to a relaxation distance, assuming a convection velocity that is some fraction of the free stream velocity. The relaxation time is presently unknown, but can be estimated by fitting an appropriate model to the near-slot data.

These ideas can be expressed quantitatively. The relaxation process can be described as:

$$MAXDR = MAXDR_{Virk} (1 - \exp(-t/\tau)) + MAXDR_{Elong} \exp(-t/\tau), \qquad (44)$$

where τ is the relaxation time to be determined. At $t = 0$, $MAXDR = MAXDR_{Elong}$, and as $t \rightarrow \infty$, $MAXDR \rightarrow MAXDR_{Virk}$. The relationship between the two asymptotes can be derived using the assumption that the friction coefficient for elongational flow is less than or equal to the Virk asymptotic friction coefficient by a factor that depends on the Weissenberg number.

$$Cf_{Elong} = F(Wi)\, Cf_{Virk} \qquad 0 \le F(Wi) \le 1 \qquad \text{for all Wi.} \qquad (45)$$

The function $F(Wi) = F(q)$ can be selected to fit the data. These assumptions can be combined to give

$$MAXDR = MAXDR_{Virk} + (1 - F(q))(1 - MAXDR_{Virk}) \exp(-t/\tau). \qquad (46)$$

Finally, for convection downstream from the slot,

$$t = x_s/U = qc_0/\rho U^2 K, \qquad (47)$$

$$MAXDR = MAXDR_{Virk} + (1 - F(q))(1 - MAXDR_{Virk}) \exp(-qc_0/\rho U^2 K\tau). \quad (48)$$

This version of the maximum friction reduction asymptote has been incorporated in the model, with the value of τ and the specific form of F(q) to be determined by fitting the Cortana data in the near-slot region.

Figure 25 shows an implementation of this modification to the model, compared with the Cortana data taken on the GTV at ARL Penn State. The experimental data are the same as shown in the earlier Figure 24, but in this case the color coding is different, reflecting polymer injection rate rather than free stream velocity. Blue is now for q/Qs = 5; red is for q/Qs = 10, and green is for q/Qs = 20. The model has been adjusted to fit the data by adjusting τ and defining F(q). The fits shown in the figure were achieved with the relaxation time τ = 0.2 seconds and the function F(q) defined by two parameters:

$$F(q) = \exp(-((q/Qs)/15)^4). \quad (49)$$

This functional form has no theoretical significance, but gives a reasonable fit to the data. Note that the relaxation time giving a reasonable fit is 1 to 2 orders of magnitude greater than the molecular relaxation time, consistent with observations of Pogrebnyak & Ivanyuta (1998) for high concentrations of polymer.

The implication of the data, as captured in the model, is that q/Qs = 5 appears to provide very little elongation of the WSR-301 polymer in solution, whereas q/Qs = 20 appears to provide a very significant amount of elongation.

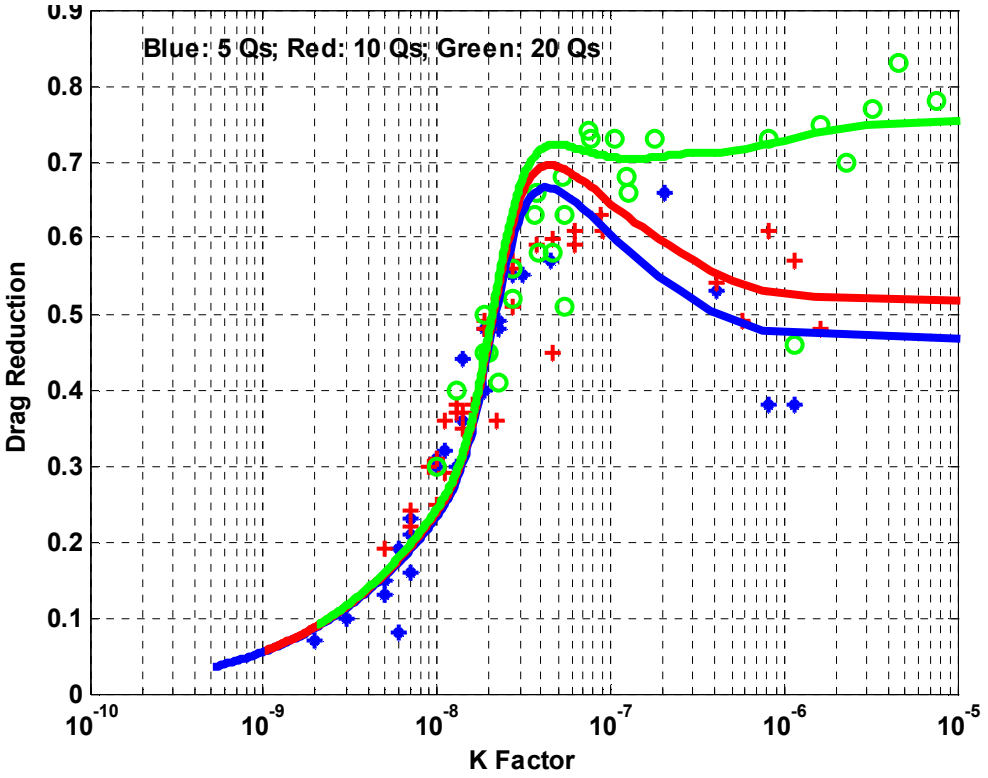

Figure 25: WSR 301 Cortana Fluidics Ejector on GTV at ARL Qs Color Coding

8 Model Limitations and Additional Research Needs

This paper has shown that a relatively simple phenomenological model can predict quite accurately the friction reduction performance of slot-ejected polymer solutions. The model contains both empirical parameters and operational parameters. The model is particularly sensitive to three of the empirical parameters; the power law exponent $\beta\beta$ that governs the approach to saturation as a function of concentration (for low concentration), the slot ejection angle expressed through the parameter α, and c_{roll}, the value of concentration at which friction reduction is reduced to half of its maximum (for high concentration). Because these parameters are both sensitive and poorly understood, additional research should focus on these three parameters.

8.1 *Improved Estimates of $\beta\beta$*

The nominal estimate $\beta\beta = 0.54$ was based on visual data extraction from a figure in a published paper. The data set was very limited and the visual extraction was probably not very accurate. The possible range for the parameter was estimated as $0.4 < \beta\beta < 0.6$.

Estimates of $\beta\beta$ can be improved by examining other data sets for which both the concentration of polymer and the velocity (or Reynolds number) are varied over a significant range and are accurately measured. Both polymer ocean experiments on smooth plates and internal flow experiments in smooth pipes should be studied.

The underlying assumptions are that (1) the approach to saturation of friction reduction follows a power law $c_0^{\beta\beta}/U_\infty^{\delta}$, where $\beta\beta \neq \delta$; (2) this power law behavior is the same for polymer ocean experiments and pipe experiments; (3) the behavior inferred from polymer ocean experiments and pipe experiments can be generalized to slot-ejected polymer experiments. These assumptions have some support. Assumption (1) appears to be one of the necessary conditions for the separation of DR vs. K curves for different values of U_∞ as observed by Winkel *et al*.

8.2 *A Model for α vs. ϕ*

Many past experiments have used ejection angles that were either less than the 7° or greater than the 20° for which Vdovin & Smol'yakov estimated α. Future experiments will also exceed those limits. A reliable means for extrapolating α would be very helpful for interpreting such experiments.

More important, if the model is to be used for engineering design, it must be capable of accurate prediction of friction reduction performance for different (especially very small) ejection angles. The goal of this research task would be to develop, from first principles, a formula to predict α as a function of ϕ. It is likely that such a formula would require a more comprehensive approach to the diffusion of polymer in the near-wall region, and might lead to deeper insights about the diffusion length, *L*, introduced by Vdovin &

Smol'yakov. In particular, it might clarify why L behaves differently for small and large ejection angles and why L appears to approach an asymptote L_{max} under some conditions.

As noted above, a critical and fundamental issue is the observation of Vdovin & Smol'yakov that, for small ejection angles, the behavior of the polymer is governed by inner variables alone, not by outer variables such as the free stream velocity. Understanding in more detail the basic physics behind this observation will be a significant advance.

8.3 *Reliable Estimate for c_{roll}*

The value of concentration for which friction reduction performance drops by ½ needs to be estimated more accurately, and the physics that produces this high-concentration roll-off needs to be better understood. The empirical data of Wu, Fruman & Tulin and of Povkh *et al* are qualitatively similar, but do not completely agree quantitatively. The functional form of the roll-off used in the model, $c_{roll}/(c + c_{roll})$, is only a rough approximation that captures the general behavior. In addition, Povkh *et al* show that the roll-off behavior depends on other parameters such as molecular weight that are not included in the present model.

9 Summary

The goal of this work was to develop a model that accurately captures the drag-reduction behavior of slot-ejected polymer in external flow and that can be used as a measure of effectiveness (MOE) for engineering purposes.

An empirical model has been developed by combining partial models from the work of earlier researchers. Models of polymer wall concentration as a function of downstream distance from the slot were taken from Vdovin & Smol'yakov (1978, 1982). A model of the dependence of friction reduction on wall concentration was inferred from data reported by Petrie *et al* (2003). Models for maximum achievable friction reduction as a function of Reynolds number were taken from Virk *et al* (1970) and from White (1991). Data on the decrease of friction reduction performance at high polymer concentration were taken from Wu, Fruman & Tulin (1977) and from Povkh *et al* (1979). These model components were combined, using simple subsidiary calculations, to create a complete model of friction reduction as a function of the dimensionless parameter K.

The complete model contains several empirical parameters from earlier published works and several operating parameters that define an experimental configuration. Each of the parameters was tested for its impact on the model. It was found that the model was very sensitive to three parameters in particular: the power law exponent that governs the approach to saturation as a function of polymer concentration, the ejection angle of the slot that extrudes the polymer into the flow, and the roll-off concentration at which performance decreases for high polymer concentrations. The power law parameter controls the slope of the DR vs. K curve in the end diffusion region. The ejection angle controls the extent of the intermediate diffusion region, and, consequently, has a major impact on overall performance. The high-concentration roll-off parameter controls behavior close to the ejection slot where initial polymer concentration is high.

For large values of K (regions near the slot) performance is generally controlled by the Virk asymptote and the high concentration roll-off. For small values of K, performance is controlled by the end diffusion zone. Between these two limits, performance *may* be controlled by the intermediate diffusion zone. However, for large ejection angles, the width of the intermediate zone becomes insignificant, and performance transitions directly from the Virk asymptote region to the diffusion far zone region. The intermediate diffusion zone is important only for small ejection angles.

The model was fine-tuned and compared with data from published experiments. Excellent agreement with data from Winkel *et al* was demonstrated. In particular, differential performance due to different free stream velocities and to different polymer types was predicted accurately. Models of friction reduction performance at shallow ejection angles produced good agreement with data taken at ARL, Penn State for Cortana Corporation. An adjunct model was developed to explain anomalous behavior in the near-slot region.

Limitations of the model were discussed. Three areas of high priority research were identified: (1) more accurate estimation of the power law parameter for the low-concentration approach to saturation and the roll-off parameter for high concentration; (2) a first principles model of the effect of changing the ejection angle; (3) additional modeling of near-slot behavior of dilute polymer solutions, considering the effects of concentration and molecular weight.

The model provides a useful MOE tool for evaluation of field experiments and for design of slot ejector systems. The local DR vs. K curves can be inverted to predict local DR vs. downstream distance. That function can then be integrated to predict total friction reduction as a function of polymer consumption for various slot designs. Performance for single slots or multiple slots can be evaluated and compared. In this way, an optimum polymer ejection system can be developed, its performance can be evaluated, and its cost/effectiveness vis-à-vis reduced fuel consumption can be determined.

10 References

Dua, A. & Cherayil, B. J., Chain dynamics in steady shear flow. *J. Chem. Phys*. **112**(19), 8707-8714, (2000)

Dua, A. & Cherayil, B. J., Effects of stiffness on the flow behavior of polymers. *J. Chem. Phys*. **113**(23), 10776-10783, (2000)

Dua, A. & Cherayil, B. J., Polymer dynamics in linear mixed flow. *J. Chem. Phys*. **119**(11), 5696-5700, (2003)

Gyr, A. & Brewersdorff, H. W., *Friction reduction of Turbulent Flows by Additives*, Kluwer Academic Publishers, Dordrecht, 1995

Hatfield, J. W. & Quake, S. R., Dynamic properties of an extended polymer in solution. *Phys. Rev. Lett*. **82**(17), 3548-3551, (1999)

Hur, J. S., Shaqfeh, E. S. G., Babcock, H. P. & Chu, S., Dynamics and configurational fluctuations of single DNA molecules in linear mixed flows. *Phys. Rev. E* **66**, 010915, (2002)

Larson, R. G., Perkins, T. T., Smith, D. E. & Chu, S., Hydrodynamics of a DNA molecule in a flow field. *Phys. Rev. E* **55**(2), 1794-1797, (1997)

LeDuc, P., Haber, C., Bao, G. & Wirtz, D., Dynamics of individual flexible polymers is a shear flow. *Nature* **399**, 564-566, (1999)

Perkins, T. T., Quake, S. R., Smith, D. E. & Chu, S., Relaxation of a single DNA molecule observed by optical microscopy. *Science* **264**, 822-826, (1994)

Perkins, T. T., Smith, D. E. & Chu, S., Direct observation of tube-like motion of a single polymer chain. *Science* **264**, 819-822, (1994)

Perkins, T. T., Smith, D. E., Larsen, R. G. & Chu, S., Stretching of a single tethered molecule in a uniform flow. *Science* **268**, 83-87, (1995)

Perkins, T. T., Smith, D. E. & Chu, S., Single polymer dynamics in an elongational flow. *Science* **276**, 2016-2021, (1997)

Petrie, H., Deutsch, S., Fontaine, A., Brungart, T., Polymer friction reduction with surface roughness in flat-plate turbulent boundary layer flow. *Experiments in Fluids* **35**, 8-23, (2003)

Pogrebnyak, V. G. & Ivanyuta, Y. F., Experimental research of the influence of conditions of polymer admission to the boundary layer on a drop of turbulent friction. Proceedings of the Rhode Island Conference on Friction reduction, July 1998

Povkh, I. L., Pogrebnyak, V. G. & Toryanik, A. I., Relation between molecular structure of polyethylene oxide solutions and friction reduction. *Inzhenerno-Fizicheskii Zhurnal* **37**(4), 581-588, (1979) English translation: Plenum Publishing Corporation UDC 532.73:547.963.3:517.4 (1980)

Quake, S. R., Babcock, H, & Chu, S., The dynamics of partially extended single molecules of DNA. *Nature* **388**, 151-154, (1997)

Schlichting, H., *Boundary Layer Theory*, 4th ed., McGraw Hill, New York, (1960)

Schroeder, C. M., Babcock, H. P., Shaqfeh, E. S. G., & Chu, S., Observation of polymer conformation hysteresis in extensional flow. *Science* **301**, 1515-1519, (2003)

Smith, D. E., Perkins, T. T. & Chu, S., Self diffusion of an entangled DNA molecule by reptation. *Phys. Rev. Lett*. **75**(22), 4146-4149, (1995)

Smith, D. E., Perkins, T. T., & Chu, S., Dynamical scaling of DNA diffusion coefficients. *Macromolecules* **29**, 1372-1373, (1996)

Smith, D. E. & Chu, S., Response of flexible polymers to a sudden elongational flow. S*cience* **281**, 1335-1340, (1998)

Smith, D. E., Babcock, H. P. & Chu, S., Single polymer dynamics is steady shear flow. S*cience* **283**, 1724-1727, (1999)

Vdovin, A. & Smol'yakov, A., Diffusion of polymer solutions in a turbulent boundary layer. *Zh. Prikl. Mekh. Tekh. Fiz*. **2**, 66-73, (1978)

Vdovin, A. & Smol'yakov, A., Turbulent diffusion of polymers in a turbulent boundary layer. *Zh. Prikl. Mekh. Tekh. Fiz*. **4**, 98-104, (1981)

Virk, P. S. & Baher, H., The effect of polymer concentration on friction reduction. *Chem. Eng. Sci*. **25**, 1183-1189, (1970)

Virk, P. S., Mickley, H. S. & Smith, K. A., The ultimate asymptote and mean flow structure in Toms phenomenon. *Trans. ASME Journal of Applied Mechanics* 488-493, (1970)

White, F. M., *Viscous Fluid Flow*, McGraw Hill, New York, (1991)

Winkel, E. S., Oweis, G., Vanapilli, S. A., Dowling, D. R., Perlin, M., Solomon, M. J., & Ceccio, S. L., Friction friction reduction at high Reynolds numbers with wall ejected

polymer solutions. *Proc. 26th Symposium on Naval Hydrodynamics*, Rome, September 2006

Wu, J. & Tulin, M. P., Friction reduction by ejecting additive solutions into pure-water boundary layer. *Trans. ASME Journal of Basic Engineering*, **94**, 749-754, (1972)

Wu, J., Fruman, D. H. & Tulin, M. P., Friction reduction by polymer diffusion into a pure-water boundary layer at high Reynolds numbers. *Proc. Second International Conference on Friction reduction*, August 31-September 2, 1977

11 Glossary

Alpha- Alpha (α) is a parameter that depends on angle at which the ejectant is introduced into the free stream flow.

Beta - Beta (β) is a parameter that depends on the ejection angle of the slot. $\beta = 1 - \alpha$ to ensure that $c_w/c_0 = 1/e$ when $x = L$, defined as the diffusion length.

Boundary Layer - The boundary layer (**BL**) is defined as the region in an external flow where the velocity varies from zero at the wall to approximately 99 percent of the free stream velocity. It is the region where the effects of fluid viscosity (η) are present.[1]

Buffer Layer - The region where both viscous and Reynold's stresses are comparable[2] (also referred to as transition layer).

Correction Factor - The correction factor (**F**) is a factor to correct for the maximum diffusion length (L_{max}) and is given by the equation: $F = \dfrac{kqc_0 \big/ \rho U_\infty L_{max}}{1 - e^{\frac{-kqc_0}{\rho U_\infty L_{max}}}}$

Delta - In this context, the parameter delta (δ) is the power law exponent that describes the contribution of the velocity in the approach to saturation as a function of wall concentration.

Density - The mass per unit volume is represented by the Greek letter rho (ρ). For seawater, its mass density at 28.3 ^oC, $\rho = 1022.2$ kg/m^3.

Diffusion Length - The diffusion length (***L***) as defined by Vdovin and Smol'yakov is the downstream distance at which the wall concentration has dropped to 1/e of its initial value (where e is the base of the natural logarithm).

Double Beta - The parameter double beta ($\beta\beta$) is the power law exponent of the concentration in the approach to saturation from lower concentrations. Numerically, it is a constant having a value of less than one.

Downstream Distance - The downstream distance, denoted by the term (**x**) is relative to the virtual origin such that $x = x_o + x_s$ when x_o is the coordinate of the slot, and x_s is the downstream distance from the slot.

---

[1] Gillmer, Thomas C. and Bruce Johnson, Introduction to Naval Architecture, Naval Institute Press, Annapolis, MD, 1982, pg 216.

[2] Tennekes, H. and J.L. Lumley, A First Course in Turbulence, the MIT Press, Cambridge, MA and London, England, 16th printing 1997, pg 161.

Friction reduction - For this paper, friction reduction will refer to a reduction of the skin friction drag which is caused by shear stresses at the surface. Again, for this paper, the reduction in skin friction drag is attained via polymer ejection.

Dynamic Viscosity - "A measure of the resistance to flow of a fluid under an applied force"[3] denoted by the Greek symbol mu ($\mu = \nu\rho$).

Ejection Angle - The angle, usually measured in degrees, at which the ejected solute is introduced into the free stream via the ejector. This angle (ϕ) is typically measured as the angle between the upstream free stream surface and the upstream ejector surface.

Ejection Velocity - The velocity at which the solute is ejected from the ejection orifice into the free stream ($\mathbf{u_{ej}}$).

Far Zone - As the turbulent boundary layer (TBL) thickens downstream from the point of ejection, diffusion continues to reduce the concentration of solute near the wall, but the rate is algebraic rather than exponential. On the K-Plot, the Far Zone is also the region of changing slope to the left of the constant-slope region, approaching zero drag as K decreases. The Far Zone is also sometimes referred to as the Final Zone or End Zone.

Gamma - The term gamma (γ) is a constant that depends on the flow velocity. The parameter γ appears in the exponent that governs the approach to saturation as a function of wall concentration. In general, increasing γ increases the apparent performance of the polymer.

Initial Concentration – Typically refers to the concentration of the polymer powder in the fluid being ejected on a weight basis. The initial concentration is often denoted by the symbols $\mathbf{c_0}$ or $\mathbf{C_i}$ and is usually described in weight parts per million (**wppm**).

Initial Zone - Located very close to the slot, where the polymer is confined to the near-wall region and the wall concentration remains close to the initial concentration. Typically, the Initial Zone is very short.

Intermediate Zone - In this zone, the diffusion process transports the solute (in this case, the polymer additive) away from the wall until it occupies much of the turbulent boundary layer. The concentration of the solute at the wall decreases exponentially in this region or zone. The Intermediate Zone is also sometimes referred to as the Transition Zone.

k_0 - Performance factor for polymer as derived from Vdovin and Smol'yakov's seminal work. They established a method for comparing DR results that used different types of polymers. The reference value for which $\mathbf{k_0}$ is equivalent to one (1) is Dow Chemical's PEO (PolyEthylene Oxide) WSR-301.

[3] http://dictionary.reference.com/browse/dynamic%20Viscosity

k - This term is derived from the reference k_0. Polymers that have twice as much ability to provide DR as WSR-301 would have a **k**-value of two (2) and polymers that were only ½ as efficient as WSR-301 would have a k-value of 0.5.

K-Curve - A curve plotted on a K-factor graph which usually has the K-factor plotted logarithmically on the x-axis (abscissa) and % DR (specifically, this is percentage friction reduction, not percentage drag reduction) linearly plotted on the y-axis (ordinate).

K-Factor - A value based on the work by Vdovin & Smol'yakov $\left[K - Factor = \frac{Q \times C_i}{\rho \times U_\infty \times X_{te}} \right]$ where Q = the ejection mass flow rate (cm^2/sec), C_i = the ejectant concentration (g/cm^3), ρ = the density of the fluid medium (g/cm^3), U_∞ = the velocity of the external flow (cm/sec), and X_{te} = the distance from the ejection slot to the trailing edge of the drag balance (cm).

Kinematic Viscosity - This is a coefficient which describes the diffusion of momentum.[4] The kinematic viscosity (**ν**) is calculated taking the *dynamic viscosity* (viscosity coefficient that determines the dynamics of incompressible Newtonian fluid) and dividing by the density of Newtonian fluid $\left[\upsilon = \frac{\eta}{\rho} \right]$.[5]

Laminar Flow - "Sometimes known as streamline flow, occurs when a fluid flows in parallel layers, with no disruption between the layers. In fluid dynamics, laminar flow is a flow regime characterized by high momentum diffusion, low momentum convection, pressure and velocity independent from time. It is the opposite of turbulent flow. In nonscientific terms laminar flow is *smooth*, while turbulent flow is *rough*."[6] "In laminar flow, the fluid moves in smooth layers or lamina. There is relatively little mixing and consequently the velocity gradients are small and shear stresses are low. The thickness of the laminar boundary layer increases with distance from the start of the boundary layer and decreases with Reynolds number."[7]

Length - The measure of the greatest dimension of a plane or solid figure often denoted by the symbol (**L**) and is usually in units of ft, meters, etc.

Length of the Plate - The length of the plate ($\mathbf{L_p}$) refers to a surface with an infinite extent in the direction perpendicular to the flow. The surface may be either a flat plate or a body of revolution having length, L_p.

Maximum Friction Reduction - For a specific case (i.e. ejector type, solute flow rate, external velocity, , this is the maximum amount of friction reduction that was attained.

[4] http://scienceworld.wolfram.com/physics/KinematicViscosity.html
[5] http://en.wikipedia.org/wiki/Kinematic_Viscosity
[6] http://en.wikipedia.org/wiki/Laminar_flow
[7] http://www.desktopaero.com/appliedaero/blayers/blayers.html

Reynolds Number - The Reynolds number (**Re**), refers to "the ratio of inertial forces ($v_s\rho$) to viscous forces (μ/L) and consequently it quantifies the relative importance of these two types of forces for given flow conditions."[8]

Roll-off Parameter - An empirical parameter for high-concentration effects that denotes the movement of solute from an area of higher concentration near the wall to an area of lower concentration further out into the boundary layer ($\mathbf{c_{roll}}$).

Saturation - The non-linear approach of a dependent variable to a fixed asymptote as an independent variable increases linearly. In this paper, the terminology as applied to the approach of friction reduction to its maximum value as polymer concentration increases.

Slot Width - The slot width refers to the ejector orifice as measured from the upstream side of the ejector opening to the downstream side of the ejector ($\mathbf{w_s}$). Ejectors widths are typically on the order of 1 mm across.

Tau – The term tau (τ) refers to the relaxation time of the polymer molecule.

Toms Effect - In 1949, the British researcher B.A. Toms discovered that dissolving small quantities of heavy, long-chain molecular polymers in a solution reduced the drag in a turbulent flow by upwards of 70 percent.

Turbulent Flow - "In fluid dynamics, turbulence or turbulent flow is a flow regime characterized by chaotic, stochastic property changes. This includes low momentum diffusion, high momentum convection, and rapid variation of pressure and velocity in space and time."[9]

Turbulent Boundary Layer - "The turbulent boundary layer (**TBL**) flow is characterized by unsteady mixing due to eddies at many scales. The result is higher shear stress at the wall, a "fuller" velocity profile, and a greater boundary layer thickness. The wall shear stress is higher because the velocity gradient near the wall is greater. This is because of the more effective mixing associated with turbulent flow. However, the lower velocity fluid is also transported outward with the result that the distance to the edge of the layer is larger."[10]

Velocity - A vector quantity whose magnitude is a body's speed and whose direction is the body's direction of motion.[11] Referred to as ($\mathbf{U_{ref}}$) with the units kts, ft/sec, or m/sec and can also refer to the free stream velocity ($\mathbf{U_\infty}$).

Viscous Sublayer - This term refers to a zone of unsteady flow where velocity fluctuations do not contribute much to the total stress due to the overwhelming effects of viscosity.[12]

---

[8] http://en.wikipedia.org/wiki/Reynolds_number
[9] http://en.wikipedia.org/wiki/Turbulent_flow
[10] http://www.desktopaero.com/appliedaero/blayers/blayers.html
[11] http://dictionary.reference.com/browse/velocity
[12] Tennekes, H. and J.L. Lumley, A First Course in Turbulence, the MIT Press, Cambridge, MA and London, England, 16th printing 1997, pg 160.

Virtual Origin - Denoted as the position (**x**) along the plate at which the turbulent boundary layer begins. The virtual origin is assigned the coordinate x = 0, and downstream positions are referenced to that origin.

Volume Ejection Rate per Unit Span - This term is the volume discharge per unit span width flow rate of the ejected additive (solute) into the surrounding fluid medium (typically sea water in an at-sea experiment) and is denoted in units of quanta of viscous sublayer volume flow rates [viscous sublayer flow rate $0<y+\leq 11.6$ and is = 67.3ν in ft^3/sec or m^3/sec].[13] This term for the volume ejection rate per unit span is often denoted by either the symbol $\mathbf{Q_s}$ or **q**.

Weissenberg Number – "A dimensionless number used in the study of viscoelastic flows. It is named after Karl Weissenberg. The dimensionless number is the ratio of the relaxation time of the fluid and a specific process time. For instance, in simple steady shear, the Weissenberg number, often abbreviated as **Wi** or We, is defined as the shear rate times the relaxation time ($Wi = \gamma\lambda$). Since this number is obtained from scaling the evolution of the stress, it contains choices for the shear or elongation rate, and the length-scale. Therefore the exact definition of all non dimensional numbers should be given as well as the number itself."[14]

[13] Fontaine, A.A., H.L. Petrie, and T.A. Brungart, "Velocity Profile Statistics in a Turbulent Boundary Layer with Slot-Injected Polymer" Journal of Fluid Mechanics (1992), vol. 238, pp 435-466.
[14] http://en.wikipedia.org/wiki/Weissenberg_number